

Excitons in quasi-one-dimensional organics: Strong correlation approximation

Z. G. Yu, A. Saxena, and A. R. Bishop

Theoretical Division, Los Alamos National Laboratory, Los Alamos, New Mexico 87545

(Received 5 February 1997; revised manuscript received 17 April 1997)

An exciton theory for quasi-one-dimensional organic materials is developed in the framework of the Su-Schrieffer-Heeger Hamiltonian augmented by short-range extended Hubbard interactions. Within a strong electron-electron correlation approximation, the exciton properties are extensively studied. Using scattering theory, we analytically obtain the exciton energy and wave function and derive a criterion for the existence of a B_u exciton. We also systematically investigate the effect of impurities on the coherent motion of an exciton. The coherence is measured by a suitably defined electron-hole correlation function. It is shown that, for impurities with an on-site potential, a crossover behavior will occur if the impurity strength is comparable to the bandwidth of the exciton, corresponding to exciton localization. For a charged impurity with a spatially extended potential, in addition to localization the exciton will dissociate into an uncorrelated electron-hole pair when the impurity is sufficiently strong to overcome the Coulomb interaction which binds the electron-hole pair. Interchain coupling effects are also discussed by considering two polymer chains coupled through nearest-neighbor interchain hopping t_{\perp} and interchain Coulomb interaction V_{\perp} . Within the t matrix scattering formalism, for every center-of-mass momentum, we find two poles determined only by V_{\perp} , which correspond to the interchain excitons, and four poles only involving intrachain Coulomb V , which are intrachain excitons. The interchain exciton wave function is analyzed in terms of inter- and intra-chain character. Finally, the exciton state is used to study the charge transfer from a polymer chain to an adjacent dopant molecule. From a variational wave function for the total system, we explore the dependence of the probability of charge transfer on the acceptor level, the hopping, and the wave function of the exciton. [S0163-1829(97)00531-6]

I. INTRODUCTION

In recent years, the exciton concept of electron-hole bound states has gained popularity in conjugated organic polymers. Experimentally, it has been discovered that poly(phenylene vinylene) (PPV) and its derivatives, e.g., poly[2-methoxy, 5-(2' ethyl-hexoxy)-1,4 phenylene vinylene] (MEH-PPV) can be used as the active luminescent layer in electroluminescent light-emitting diode devices.¹ By using different conjugated polymers, polymer light-emitting diodes (PLED) have been fabricated which emit throughout the visible region of the spectrum.¹⁻⁶ It is believed that radiative recombination of excitons gives rise to luminescence, so a comprehensive understanding of exciton properties in polymer chains is very important to guide improvements in quantum efficiency of these PLED devices. Also, conjugated polymers have shown potential application in photonics for their large optical nonlinearity and ultrafast response time.^{7,8} In view of the significant role excitons play in optical properties of a system, a detailed study of the exciton is also an important issue for polymer photonic device design. Theoretically, excitons in conjugated polymers are both attractive and challenging because of the coexistence of low-dimensional confinement and strong electron-electron ($e-e$) correlation in these systems. These ingredients have in fact led to many controversies during the study of excitons in polymers.⁹⁻¹²

Discussion of excitons in solids can be traced back more than half a century to the pioneering work by Frenkel¹³ which even preceded the band theory in solids. After numerous studies on excitons over several decades, the exciton, as an elementary excitation, has been well established in bulk

insulators. This is the reason why in the existing exciton theories for polymers,¹⁴⁻¹⁷ the standard exciton theory in semiconductors¹⁸ was usually borrowed with limited justification. In these theories, the polymer is regarded as a Peierls insulator which means the gap between the conduction and valence bands arises from the Peierls dimerization, a well-known nesting effect in one-dimensional metals.¹⁹ Then the exciton states are solved considering the $e-e$ interaction as a perturbation as in traditional exciton theory. But the polymer is significantly different from the conventional semiconductor. In a semiconductor, the electron correlation effects can largely be neglected and it is plausible to treat the $e-e$ interaction as a perturbation. However, the polymer is typically a strongly correlated system with a moderate to large on-site Hubbard repulsion, and much of the band gap is due to the electron correlation rather than the dimerization.²⁰⁻²³ Thus the foundation of existing exciton theories in conjugated polymers is not so firm, and these theories have already led to some qualitatively incorrect results. For example, from these theories, the $1B_u$ exciton is lower than the $2A_g$, but typically the order should be reversed. Again, the threshold of the conduction band is independent of U , the on-site Hubbard repulsion.¹⁷ This is unreasonable since, when an electron is excited to the conduction band, double occupation must occur and cause an additional Hubbard repulsion.

Having appreciated the central importance of electron correlation in polymers, several efforts have been undertaken to take account of the strong correlation effect on exciton states.²⁴⁻²⁸ In these works, numerical exact diagonalization and density matrix renormalization group (DMRG) approaches are employed to handle small systems. From those numerical results, some useful information on the electron

structure of the polymer can be captured by extrapolating the results to a long chain. However, these works cannot be regarded as constituting an exciton theory, since only some specific states are focused on in the calculations and the exciton is not treated as a quasiparticle. We must seek a more complete exciton theory of conjugated polymers, in which the correlation is stressed and the exciton is an elementary excitation. This kind of theory will then be useful to study the optical and transport properties related to the exciton. In this paper, we will develop an exciton theory in the limit in which the Hubbard U is the main origin of the band gap (i.e., the polymer is regarded as a Mott insulator). In this regime, the spin has little effect on the exciton states and the energy difference between the singlet and triplet states is negligibly small compared with their binding energies. Using scattering theory, we will analytically calculate the exciton states and find a critical strength of the e - e interaction for the existence of bound exciton states.

Currently, chemically synthesized polymers cannot be free from impurities and the “pristine” samples of polymers contain a non-negligible density of impurities and defects from the cross-linking, complex morphological effects, conjugation length effects, and some extrinsic defects. Such impurities sometimes critically influence the properties of the system, e.g., the transport. For example, the conductivity in *trans*-polyacetylene can be dramatically enhanced by 13 orders of magnitude by doping.⁷ In an impurity-free system, the exciton states with different center-of-mass momenta form exciton bands, and within the band the exciton moves coherently as a composite particle. The disorder tends to produce localized states, and in one-dimensional systems, any nonvanishing impurity potential will lead to a localized electronic state.²⁹ Thus it is interesting to examine the localization of an exciton, a composite particle, due to the impurities, and furthermore to determine if the exciton ceases to be a composite particle of electron and hole when the impurity is strong enough. In this paper, we will address the interplay of coherent motion of the exciton and different types of impurities in our conjugated polymer model.

Strictly speaking, the polymer is only a quasi-one-dimensional system, in which interchain couplings always exist, and sometimes their effects are striking. Many calculations have shown that nonlinear excitations like solitons and polarons may be unstable by taking the interchain coupling into account.^{30,31} Recently, great attention has been paid to the interchain effects in luminescent polymers, since many experiments demonstrated that a large fraction of primary photoexcitations are interchain excitons or polaron pairs.^{32–34} Also some theoretical calculations have been carried out to explore the interchain coupling effects on exciton properties.^{35,36} Although the terminology of interchain exciton and intrachain exciton are widely used in current literature, these concepts are not so clearly delineated. From the principles of quantum mechanics, the wave function of every eigenstate in the coupled system must be distributed over the whole system, so it is difficult to distinguish from the wave function which one corresponds to the interchain and which one to the intrachain exciton. We will clarify what the interchain and intrachain exciton states are and calculate their energies and wave functions.

Photoconductivity in conjugated polymers can sometimes

be greatly enhanced by intercalating or doping the polymer with a particular species of molecule. Interesting examples of this phenomenon occur when MEH-PPV is doped by fullerene C_{60} molecules.^{37,38} This is because the exciton, the bound electron and hole state in the polymer, will decay when the dopant molecule is introduced. The electron (or hole) in the exciton will transfer from the polymer chain to the doped molecule, giving rise to a free carrier. Rice and Gartstein recently proposed a theory to explain the ultrafast time scale for this charge transfer.³⁹ From a quantum mechanics perspective, assuming we have an exciton state in the polymer chain due to photoexcitation, when the coupling between the chain and the molecule is switched on, the electron will move in the whole system (including the chain and the molecule), and this state must have a lower energy than the initial state. So another point of view from which to study the charge transfer is to ask what percentage of the electron (hole) has transferred from the polymer chain to the dopant. This percentage should depend on the acceptor level and the coupling between the chain and the molecule, as well as the initial exciton wave function in the polymer chain. We will discuss this issue here.

The paper is organized as follows. First, we develop an exciton theory for conjugated polymers in the strong correlation (large Hubbard U) approximation in Sec. II. In Sec. II A we simplify a Peierls-extended Hubbard model to a model represented by spinless fermions with short-range e - e interactions in real space. Then we use t matrix scattering theory to determine the wave function and binding energy of exciton states analytically and derive a criterion for the existence of the B_u exciton in Sec. II B. This criterion is further proved according to the Levinson’s theorem in scattering theory in Sec. II C. In Sec. II D a more formal and compact formalism for optical absorption in conjugated polymers is presented based on our exciton theory in the large- U limit. Section III is devoted to the impurity effects on the coherent motion of the exciton. Using a suitably defined electron-hole correlation function, we study different types of impurity. In Sec. IV, we investigate interchain coupling effects by considering a two-chain system supplemented by nearest-neighbor interchain hopping t_{\perp} and interchain e - e interaction V_{\perp} . Using the t matrix formalism, we analytically determine the poles corresponding to intrachain and interchain excitons, respectively. We also show the wave function of the interchain exciton. In Sec. V, the static A_g and B_u excitons are used to study the charge transfer in a molecularly doped polymer. By constructing a variational wave function for the whole system, the energy of this variational state, and accordingly the probability of charge transfer, can be obtained. Finally, we summarize our results in Sec. VI.

II. AN EXCITON THEORY IN CONJUGATED POLYMERS

In existing theories, the polymer is regarded as a Peierls insulator, and then the exciton state is determined by treating the e - e interaction (including the on-site Hubbard interaction) as a perturbation. In this picture, the single particles (electron and hole) are defined based on a noninteracting Su-Schrieffer-Heeger model, so the band gap, from these theories, is independent of the e - e interaction. In a strongly

correlated system, the electronic states are quite different from the noninteracting model. Since the ground state is half filled, an electron excited to the conduction band must cost the additional Hubbard repulsion energy caused by the double occupation. In conjugated polymers and related organic conductors, it is now accepted that the origin of the band gap comes typically from the Hubbard repulsion rather than the Peierls dimerization. So the Hubbard term should be given priority when one develops an exciton theory. In this section, we will regard the polymer as a Mott insulator and develop the exciton theory in the large- U limit. In this energy regime, double and higher order electron-hole excitations can be neglected because of their high energies ($\geq 2U$), and a single configuration interaction approximation is reasonable in determining exciton states. Before carrying out the calculation, let us recall how large the Hubbard U (in units of electronic hopping energy t) is in real systems: $U/t \sim 3-4$ in conjugated polymers and $U/t \sim 8-10$ in segregated stack charge transfer salts.^{40,41} Strictly, this strong correlation limit is applicable only when $U \gg t$, thus real conjugated polymers only marginally satisfy this approximation.

A. Hamiltonians

The theoretical model we consider is the Peierls-extended Hubbard model, i.e., the Su-Schrieffer-Heeger⁷ model augmented by an extended Hubbard interaction. For a one-dimensional chain, this model Hamiltonian is

$$H = -t \sum_{l\sigma} [1 - (-1)^l \delta] (c_{l\sigma}^\dagger c_{l+1\sigma} + \text{H.c.}) + U \sum_l n_{l\uparrow} n_{l\downarrow} + V \sum_l (\rho_l - 1)(\rho_{l+1} - 1). \quad (2.1)$$

Here $c_{l\sigma}^\dagger$ creates an electron of spin σ on site l , t is the one-electron hopping integral, δ is a bond-alternation parameter, U and V are, respectively, the on-site and nearest-neighbor Coulomb interaction, $n_{l\sigma} = c_{l\sigma}^\dagger c_{l\sigma}$ is the number operator, and $\rho_l = n_{l\uparrow} + n_{l\downarrow}$. Since we will be concerned only with electronic excitations in this work, we consider a rigid dimerized ground state as a starting point, and do not specify its explicit origin (e.g., $e-e$ interactions, electron-phonon couplings, or crystal structure). Strictly speaking, this Peierls-extended Hubbard model is directly applicable only to *trans*-polyacetylene. However, recent calculations have shown that the primary excitation in luminescent polymers like PPV can also be described within an effective linear chain model.²⁶ In these luminescent polymers, the lowest excitonic wave function extends over several repeat units. The properties of exciton are therefore not very sensitive to the detailed structure within the unit cell. From the viewpoint of renormalization, we can map the complex structure of a luminescent polymer into an effective Peierls-extended Hubbard system with the same significant physical properties by integrating out the superfluous degrees of freedom caused by the complicated unit cell structure. We have also neglected lattice relaxation, since many experiments and theories have demonstrated that $e-e$ interactions dominate electron-lattice interactions in many luminescent polymers.⁴²⁻⁴⁵ This simplification enables us to handle $e-e$ interactions in long chains

and arrive at an understanding of *electronic states* in conjugated polymers without loss of essential physics, although the quantitative explanation of some *lattice* property like vibronic structure or bond length should, indeed, take into account lattice relaxation effects.⁴⁶

To emphasize the electron correlation, we begin with the Hubbard model

$$H_0 = -t \sum_{l\sigma} (c_{l\sigma}^\dagger c_{l+1\sigma} + \text{H.c.}) + U \sum_l n_{l\uparrow} n_{l\downarrow}. \quad (2.2)$$

Although the exact wave function and the ground-state energy of this Hamiltonian have been obtained by Lieb and Wu,⁴⁷ the Green's function and correlation functions are difficult to calculate directly by using the exact wave function, and it is also difficult to use their solution to study the exciton. As a practical alternative, here we make the strong correlation (large- U) approximation. In this approximation, as we will see later, the band gap is essentially U , which is not the same as the exact solution for the Hubbard model by Lieb and Wu,⁴⁷ where the charge excitation gap is $U - 4t + \sum_{n=1}^{\infty} (-1)^n [\frac{1}{2}nU - (t^2 + \frac{1}{4}n^2U^2)^{1/2}]$. However, for the strong correlation limit $U \gg 4t$, this difference is not important, and does not affect the exciton trends we wish to establish.

The density product $n_{l\uparrow} n_{l\downarrow}$ can be expressed by the on-site electron number and spin operator, and the Hubbard model is rewritten as

$$H_0 = -t \sum_{l\sigma} (c_{l\sigma}^\dagger c_{l+1\sigma} + \text{H.c.}) + U \sum_l [\frac{1}{2}\rho_l - (-1)^l \mathbf{S}_l \cdot \mathbf{n}_l], \quad (2.3)$$

where \mathbf{S}_l is the electron spin operator at site l ,

$$\mathbf{S}_l = \frac{1}{2} \sum_{\sigma\sigma'} c_{l\sigma}^\dagger \boldsymbol{\sigma}_{\sigma\sigma'} c_{l\sigma'}, \quad (2.4)$$

and \mathbf{n}_l is a unit vector along the spin polarization axis of the electron.⁴⁸

When $U \gg t$, the ground state is expected to have Néel order. We make an approximation by assuming that \mathbf{n}_l always coincides with the z axis, which implies that the spin excitations have been ignored. Thus, in this approximation, the singlet and triplet excitons have the same energy and are not distinguishable. This is reasonable since for a one-dimensional Hubbard model, the spin and charge excitations are separated when $U \rightarrow \infty$ and by order U/t for $U \gg t$, and the exciton is a charge excitation. This point is also directly justified by comparing energies of the singlet and triplet states obtained from a finite chain exact diagonalization calculation.⁴⁹

$$H_0 \approx -t \sum_{l\sigma} (c_{l\sigma}^\dagger c_{l+1\sigma} + \text{H.c.}) + \frac{U}{2} \sum_{l\sigma} [1 - (-1)^l \sigma] c_{l\sigma}^\dagger c_{l\sigma}. \quad (2.5)$$

This Hamiltonian is readily diagonalized by introducing

$$c_{l\sigma} = \frac{1}{\sqrt{N}} \sum_k' e^{ikl} [(u_k + \sigma p_l v_k) \alpha_{k\sigma} + p_l (u_k - \sigma p_l v_k) \beta_k]. \quad (2.6)$$

Here the prime means that the summation runs over the reduced Brillouin zone $|k| < \pi/2$ and $p_l = (-1)^l$. Then

$$H_0 = - \sum_{k\sigma}' \left[\left(E_k - \frac{U}{2} \right) \alpha_{k\sigma}^\dagger \alpha_{k\sigma} + \left(E_k + \frac{U}{2} \right) \beta_{k\sigma}^\dagger \beta_{k\sigma} \right], \quad (2.7)$$

with

$$E_k = \sqrt{\frac{U^2}{4} + \varepsilon_k^2}, \quad (2.8)$$

$$\varepsilon_k = -2t \cos k. \quad (2.9)$$

The functions u_k and v_k are

$$u_k = \frac{1}{\sqrt{2}} \sqrt{1 + \frac{|\varepsilon_k|}{E_k}} \approx \frac{1}{\sqrt{2}} \left(1 + \frac{|\varepsilon_k|}{U} \right), \quad (2.10)$$

$$v_k = \frac{1}{\sqrt{2}} \sqrt{1 - \frac{|\varepsilon_k|}{E_k}} \approx \frac{1}{\sqrt{2}} \left(1 - \frac{|\varepsilon_k|}{U} \right). \quad (2.11)$$

In the case of $U \gg t$, a localized picture is more convenient. Two spinless fermions can be defined in the lattice representation as follows:⁴⁸

$$\alpha_l = \sum_{\sigma} \theta(p_l \sigma) \sqrt{2/N} \sum_k' e^{ikl} \alpha_{k\sigma}, \quad (2.12)$$

$$\beta_l = \sum_{\sigma} \theta(p_l \sigma) \sqrt{2/N} \sum_k' e^{ikl} \beta_{k\sigma}, \quad (2.13)$$

where $\theta(x)$ is the step function. Expanded in powers of t/U , $c_{l\sigma}$ can be expressed by α_l and β_l :

$$c_{l\sigma} = \theta(p_l \sigma) \alpha_l + \theta(-p_l \sigma) p_l \beta_l + \theta(-p_l \sigma) \frac{t}{U} (\alpha_{l+1} + \alpha_{l-1}) + \theta(p_l \sigma) p_l \frac{t}{U} (\beta_{l+1} + \beta_{l-1}) + O\left(\frac{t^2}{U^2}\right). \quad (2.14)$$

If we include the bond-alternation part in our unperturbed Hamiltonian, then

$$\begin{aligned} H_0' &= H_0 + \sum_{l\sigma} (-1)^l \delta t (c_{l\sigma}^\dagger c_{l+1\sigma} + \text{H.c.}) \\ &= J \sum_l (h_l^\dagger h_l + \beta_l^\dagger \beta_l) \\ &\quad + U \sum_l \beta_l^\dagger \beta_l + \frac{J}{2} \sum_l (h_{l+2}^\dagger h_l + \beta_{l+2}^\dagger \beta_{l+2} + \text{H.c.}) \\ &\quad + \delta t \sum_l (-h_l \beta_{l+1} + h_{l+1} \beta_l - \beta_{l+1}^\dagger h_l^\dagger + \beta_l^\dagger h_{l+1}^\dagger). \end{aligned} \quad (2.15)$$

Here we have introduced the hole operator $h_l^\dagger = \alpha_l$ and $J = 2t^2/U$.

By introducing the Fourier transformations

$$h_l = \frac{1}{\sqrt{N}} \sum_k e^{ikl} h_k, \quad (2.16)$$

$$\beta_l = \frac{1}{\sqrt{N}} \sum_k e^{-ikl} \beta_{-k}, \quad (2.17)$$

we can rewrite H_0' in momentum space as

$$\begin{aligned} H_0' &= \sum_k [(J + J \cos 2k) h_k^\dagger h_k + (U + J + J \cos 2k) \beta_k^\dagger \beta_k \\ &\quad + 2i \delta t \sin k (h_k \beta_{-k} - \beta_{-k}^\dagger h_k^\dagger)]. \end{aligned} \quad (2.18)$$

Making the Bogoliubov transformation

$$\eta_k = \cos \theta_k h_k + i \sin \theta_k \beta_{-k}^\dagger, \quad (2.19)$$

$$\gamma_{-k}^\dagger = -i \sin \theta_k h_k + \cos \theta_k \beta_{-k}^\dagger, \quad (2.20)$$

Hamiltonian (2.18) can be diagonalized if the relation

$$\sin 2\theta_k = \frac{-4 \delta t \sin k}{U} \quad (2.21)$$

is satisfied, yielding

$$H_0' = \sum_k (\epsilon_k \eta_k^\dagger \eta_k + \tilde{\epsilon}_k \gamma_k^\dagger \gamma_k), \quad (2.22)$$

with

$$\epsilon_k = J(1 + \delta^2) + J(1 - \delta^2) \cos 2k, \quad (2.23)$$

$$\tilde{\epsilon}_k = U + J(1 - 3\delta^2) + J(1 + 3\delta^2) \cos 2k. \quad (2.24)$$

Operators η_k^\dagger and γ_k^\dagger create the hole and electron in the new valence and conduction band, respectively. Their lattice representations are

$$\eta_l = \frac{1}{\sqrt{N}} \sum_k e^{ikl} \eta_k, \quad (2.25)$$

$$\gamma_l = \frac{1}{\sqrt{N}} \sum_k e^{-ikl} \gamma_{-k}, \quad (2.26)$$

which can be expressed by h_l and β_l to the order of $1/U$:

$$\eta_l \approx h_l - \frac{\delta t}{U} (\beta_{l+1}^\dagger - \beta_{l-1}^\dagger), \quad (2.27)$$

$$\gamma_l^\dagger \approx \beta_l^\dagger + \frac{\delta t}{U} (h_{l+1} - h_{l-1}). \quad (2.28)$$

The intersite Coulomb interaction is necessary to bind the electron and hole. We consider the V term in the Peierls-extended Hubbard model as a scattering potential, which has the local representation

$$\begin{aligned} H_{\text{int}} &= V \sum_l (\rho_l - 1)(\rho_{l+1} - 1) \\ &= V \sum_l (h_{l+1}^\dagger h_l^\dagger h_{l+1} h_l + \beta_{l+1}^\dagger \beta_l^\dagger \beta_l \beta_{l+1} \\ &\quad - h_{l+1}^\dagger \beta_l^\dagger \beta_l h_{l+1} - \beta_{l+1}^\dagger h_l^\dagger h_l \beta_{l+1}). \end{aligned} \quad (2.29)$$

Since the main interest here is an exciton, only the interaction between the electron and hole is relevant. To order $1/U$, we have

$$H_{\text{int}}^{e-h} = -V \sum_l (\eta_{l+1}^\dagger \gamma_l^\dagger \eta_l \eta_{l+1} + \gamma_{l+1}^\dagger \eta_l^\dagger \eta_l \gamma_{l+1}). \quad (2.30)$$

B. Exciton states: t matrix theory

Since the Hamiltonian is invariant with respect to translation, the exciton states can be classified according to the total quasimomentum K . We can write the exciton wave function as

$$|\Psi_K\rangle = \sum_s B_{s,K} |\psi_{s,K}\rangle, \quad (2.31)$$

where K is the center-of-mass momentum. The basis is chosen as

$$|\psi_{s,K}\rangle = \frac{1}{\sqrt{N}} \sum_l e^{iKl} \gamma_{l+s}^\dagger \eta_l^\dagger |g\rangle, \quad (2.32)$$

representing a created electron-hole pair from the ground state $|g\rangle$ with a separation s in real space. We will determine the exciton state by using t matrix scattering theory. According to t matrix theory⁵⁰

$$\mathcal{T}(z) = \mathcal{U} + \mathcal{U} \mathcal{G}(z) \mathcal{T}(z), \quad (2.33)$$

where $\mathcal{T}(z)$ is the t matrix, $\mathcal{G}(z)$ the notation for resolvent $1/(z - H'_0)$, and \mathcal{U} the potential operator. Equation (2.33) has the formal solution

$$\mathcal{T}(z) = \mathcal{U} [1 - \mathcal{G}(z) \mathcal{U}]. \quad (2.34)$$

Using the basis of Eq. (2.32), we obtain the Green's function

$$\begin{aligned} \langle r | \mathcal{G}(z) | s \rangle &\equiv G(r-s; z) = \langle \psi_{r,K} | (z - H'_0)^{-1} | \psi_{s,K} \rangle \\ &= \frac{1}{N} \sum_k \frac{e^{ik(r-s)}}{z - (\tilde{\epsilon}_k + \epsilon_{-k+K})}. \end{aligned} \quad (2.35)$$

Here $z = E_K + i0^+$ and the potential matrix is

$$\langle s | \mathcal{U} | s' \rangle \equiv \langle \psi_{s,K} | H_{\text{int}}^{e-h} | \psi_{s',K} \rangle = -V \delta_{ss'} (\delta_{s,-1} + \delta_{s,1}). \quad (2.36)$$

The utility of Eq. (2.34) rests on the possibility of actually constructing the inverse operator $1/(1 - \mathcal{G}\mathcal{U})$. This can be achieved exactly in our case since, conveniently, the potential is of short range in the local representation. Actually, the portion of the potential \mathcal{U} containing nonzero elements forms a 2×2 submatrix under the basis Eq. (2.32),

$$\begin{pmatrix} \mathcal{U}_{-1-1} & \mathcal{U}_{-11} \\ \mathcal{U}_{1-1} & \mathcal{U}_{11} \end{pmatrix} = -V \begin{pmatrix} 1 & 0 \\ 0 & 1 \end{pmatrix}. \quad (2.37)$$

Denoting D as the determinant of $1 - \mathcal{G}\mathcal{U}$, we have

$$D(E_K) = \begin{vmatrix} 1 + G(0; E_K)V & G(-2; E_K)V \\ G(2; E_K)V & 1 + G(0; E_K)V \end{vmatrix}. \quad (2.38)$$

The determinant will vanish for some specific values of the energy, which are the energies of the localized states. Consequently, to find the energy E_K of the bound exciton state we look for the roots of

$$D(E_K) = 0. \quad (2.39)$$

Subsequently, the wave function is calculated by solving the equation

$$B_{r,K} = \sum_{st} \langle r | G(E_K) | s \rangle \langle s | \mathcal{U} | t \rangle B_{t,K}. \quad (2.40)$$

First, let us focus on the static exciton, i.e., $K=0$. In this case, the system is symmetric with respect to spatial inversion. Introducing the transformation

$$B_l^+ = \frac{1}{\sqrt{2}} (B_l + B_{-l}), \quad (2.41)$$

$$B_l^- = \frac{1}{\sqrt{2}} (B_l - B_{-l}), \quad (2.42)$$

where $B_l \equiv B_{l,K=0}$, and noticing

$$G(s-t; E_0) = G(t-s; E_0), \quad (2.43)$$

we can write the determinant D as the product of two parts:

$$D(E_0) = D_-(E_0) D_+(E_0). \quad (2.44)$$

Here

$$D_-(E_0) = 1 + [G(0; E_0) - G(2; E_0)]V \quad (2.45)$$

is for the A_g state with the wave function

$$B_l^- = -V [G(l-1; E_0) - G(l+1; E_0)] B_l^-; \quad (2.46)$$

and

$$D_+(E_0) = 1 + [G(0; E_0) + G(2; E_0)]V \quad (2.47)$$

is for the B_u state with the wave function

$$B_l^+ = -V[G(l-1; E_0) + G(l+1; E_0)]B_l^+. \quad (2.48)$$

We denote x as the exciton binding energy:

$$x = E_G - E_0, \quad (2.49)$$

where E_G is the band gap,

$$E_G = (\tilde{\epsilon}_k + \epsilon_k)|_{k=\pi/2} = U - 4\delta^2 J. \quad (2.50)$$

When $\delta=0$, E_G does not equal the exact result by Lieb and Wu.⁴⁷ However, this is not a problem for estimating correct binding energies of the exciton states, since we will directly calculate the binding energy rather than first calculating the energy of the exciton. The Green's functions are readily calculated; for $x > 0$

$$G(2l+1; E_0) \equiv 0, \quad (2.51)$$

$$G(2l; E_0) = \frac{(-1)^{l+1}}{\sqrt{x^2 + 4J(1 + \delta^2)x}} \left(\frac{1 - \sqrt{1 - u^2}}{u} \right)^{2l}, \quad (2.52)$$

with

$$u^2 = \frac{4J(1 + \delta^2)}{x + 4J(1 + \delta^2)} < 1. \quad (2.53)$$

Then, by requiring $D_-(E_0) = 0$, we obtain the binding energy of the A_g exciton as

$$x_- = \frac{V^2}{V + J(1 + \delta^2)}, \quad (2.54)$$

with corresponding wave function

$$B_{2l-1}^- = -\frac{G(2l; E_0) - G(2l-2; E_0)}{\sqrt{-2[G'(0; E_0) - G'(2; E_0)]}}, \quad (2.55)$$

$$B_{2l}^- = 0. \quad (2.56)$$

Here $G'(n; E) \equiv (d/dE)G(n; E)$.

For the B_u state, when $V > 2J(1 + \delta^2)$, the binding energy of the exciton is

$$x_+ = \frac{[V - 2J(1 + \delta^2)]^2}{V - J(1 + \delta^2)}, \quad (2.57)$$

and the wave function is

$$B_{2l-1}^+ = -\frac{G(2l; E_0) + G(2l-2; E_0)}{\sqrt{-2[G'(0; E_0) + G'(2; E_0)]}}, \quad (2.58)$$

$$B_{2l}^+ = 0. \quad (2.59)$$

When $V < 2J(1 + \delta^2)$, a solution $E_0 < E_G$ satisfying equation $D_+(E_0) = 0$ cannot be found, i.e., there is no bound state. This result gives a criterion for the existence of a B_u exciton. Finite chain numerical DMRG and exact diagonalization calculations show that the binding energy of the $1B_u$ state is

near zero when V is not large, but are not conclusive as to whether the state is strictly bound or free.⁵¹ Our analytical results clearly indicate that the stable $1B_u$ exciton does not exist when V is less than $2J(1 + \delta^2)$. Since this critical value is half of the width of the continuum band, $4J(1 + \delta^2)$, and the bandwidth describes the kinetic energy of a free particle, this criterion is a reflection of the competition between the kinetic energy and the attraction of the electron and hole.

C. Proof of the criterion: Levinson's theorem

The criterion derived above can be proven by Levinson's theorem.⁵² Namely, the number of bound states in representation s lying either above or below the continuum band can be determined by using

$$\delta_s(E_i) - \delta_s(E_f) = \pi n_s. \quad (2.60)$$

Here E_i is the lowest energy in the band and E_f the highest. n_s is number of states in any row of representation s separated from the band. δ_s is the phase shift that appears in the usual partial wave expansion for the scattering amplitude,⁵⁰ which can also be extracted from the subdeterminants of $\det(1 - \mathcal{GU})$,

$$\tan \delta_s = -\text{Im}D_s / \text{Re}D_s. \quad (2.61)$$

In the exciton case,

$$E_i = E_G, \quad (2.62)$$

$$E_f = (\epsilon_k + \tilde{\epsilon}_k)_{k=0} = E_G + 4J(1 + \delta^2). \quad (2.63)$$

It should be noted that in a one-dimensional system the density of states at the edge of the continuum band will diverge, so the form of Eq. (2.60) in our case is

$$\delta_s(E_i - 0^+) - \delta_s(E_f + 0^+) = \pi n_s. \quad (2.64)$$

The Green's functions in different energy regions can be calculated according to the definition Eq. (2.35). We give the explicit expressions in Appendix A. Then the subdeterminants D_- and D_+ are obtained by straightforward calculations.

For $E_0 = E_i - 0^+$, i.e., the energy is just below the onset of the continuum band,

$$D_- = -\infty - i0^+, \quad (2.65)$$

$$D_+ = 1 - \frac{V}{2J(1 + \delta^2)} - i0^+, \quad (2.66)$$

and the phase shifts are

$$\delta_-(E_i - 0^+) = \pi, \quad (2.67)$$

$$\delta_+(E_i - 0^+) = \begin{cases} 0, & V < 2J(1 + \delta^2) \\ \pi, & V > 2J(1 + \delta^2). \end{cases} \quad (2.68)$$

For $E_0 = E_f + 0^+$, i.e., the energy is just above the top of the continuum band,

$$D_- = 1 + \frac{V}{2J(1 + \delta^2)} - i0^+, \quad (2.69)$$

$$D_+ = +\infty - i0^+, \quad (2.70)$$

and the corresponding phase shifts are

$$\delta_-(E_f + 0^+) = 0, \quad (2.71)$$

$$\delta_+(E_f + 0^+) = 0. \quad (2.72)$$

Thus we have

$$\delta_-(E_i - 0^+) - \delta_-(E_f + 0^+) = \pi, \quad (2.73)$$

showing that there is always an A_g bound exciton for a non-vanishing V . However, when $V < 2J(1 + \delta^2)$,

$$\delta_+(E_i - 0^+) - \delta_+(E_f + 0^+) = 0, \quad (2.74)$$

indicating that there is no B_u bound exciton. The bound exciton will appear only when $V > 2J(1 + \delta^2)$, since then

$$\delta_+(E_i - 0^+) - \delta_+(E_f + 0^+) = \pi. \quad (2.75)$$

To get an overall picture of the phase shift in this one-dimensional system, we also examine the phase shifts at $E_i + 0^+$ and $E_f - 0^+$. For $E_0 = E_i + 0^+$, i.e., the energy is just above the onset of the continuum band,

$$D_- = 1 + \frac{V}{2J(1 + \delta^2)} - i\infty, \quad (2.76)$$

$$D_+ = 1 - \frac{V}{2J(1 + \delta^2)} - i0^+, \quad (2.77)$$

and the phase shifts are

$$\delta_-(E_i + 0^+) = \pi/2, \quad (2.78)$$

$$\delta_+(E_i + 0^+) = \begin{cases} 0, & V < 2J(1 + \delta^2) \\ \pi, & V > 2J(1 + \delta^2). \end{cases} \quad (2.79)$$

For $E_0 = E_f - 0^+$, i.e., the energy is just below the top of the continuum band,

$$D_- = 1 + \frac{V}{2J(1 + \delta^2)} - i0^+, \quad (2.80)$$

$$D_+ = 1 - \frac{V}{2J(1 + \delta^2)} - i\infty, \quad (2.81)$$

and the phase shifts are

$$\delta_-(E_f - 0^+) = 0. \quad (2.82)$$

$$\delta_+(E_f - 0^+) = \begin{cases} \pi/2, & V < 2J(1 + \delta^2) \\ \pi/2, & V > 2J(1 + \delta^2). \end{cases} \quad (2.83)$$

Now let us study the behavior of the phase shift as a function of energy. For the A_g state, when the energy passes through the edge of the band the phase shift falls discontinuously from π to $\pi/2$, then gradually approaches zero at the top of the band. So there is always a bound state. For the B_u exciton, when $V < 2J(1 + \delta^2)$ the phase shift increases from zero as the energy increases from the bottom of the band, and approaches $\pi/2$ just below the top of the band, and then drops to zero again when we pass through the top edge

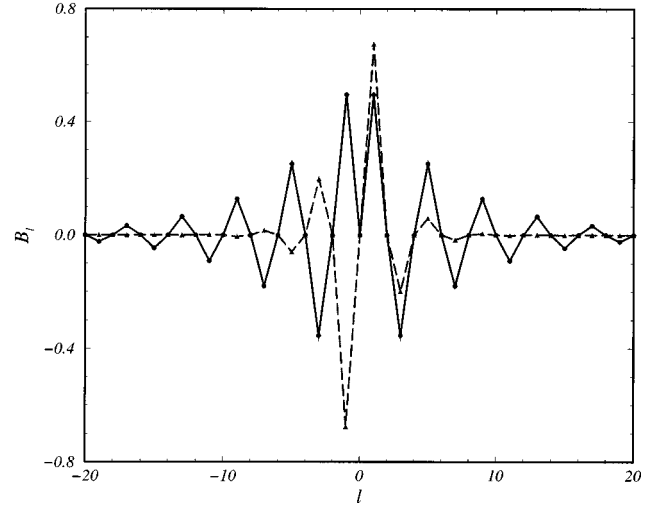


FIG. 1. Wave functions of the A_g and B_u bound exciton with $U = 10t$, $V = 0.5t$, and $\delta = 0.2$. The dashed and solid lines correspond to the A_g and B_u states, respectively.

of the band. Thus no bound state exists. When $V > 2J(1 + \delta^2)$, the phase shift decreases from π to $\pi/2$ as the energy increases from the bottom to the top of band, and abruptly falls to zero when we cross the edge of the band. Thus a bound state appears. The discontinuity of the phase shift at the band edges is due to the infinite density of states at the bottom and top of the band.

Figure 1 shows the wave functions of the A_g and B_u states with $U = 10t$, $V = 0.5t$, and $\delta = 0.2$, corresponding to binding energies $x_+ = 0.024t$ and $x_- = 0.353t$, respectively. We can see that the wave function of the A_g exciton decays more rapidly than that of the B_u one. For $x > 0$, we introduce the parameter z ,

$$z = -\ln\left(\frac{1 - \sqrt{1 - u^2}}{u}\right) > 0. \quad (2.84)$$

Since for large l ,

$$G(2l; E_0) \sim e^{-z|2l|}, \quad (2.85)$$

we can define the width R of the $K = 0$ exciton by $R = 2/z$. From Eq. (2.84), we estimate the width is about three lattice constants for the A_g exciton and about 12 lattice constants for the B_u , as shown in Fig. 1.

We calculate the energy of the exciton for $K \neq 0$ from $D(E_K) = 0$. A straightforward computation of Eq. (2.35) gives

$$G(0; E_K) = -\frac{1}{\sqrt{ac - b^2}}, \quad (2.86)$$

$$\begin{aligned} G(2; E_K) &= G^*(-2; E_K) \\ &= -\frac{1}{4b^2 + (a - c)^2} \left\{ \left[2(a - c) + \frac{c^2 - a^2}{\sqrt{ac - b^2}} \right] \right. \\ &\quad \left. + i \left[4b - \frac{2b(a + c)}{\sqrt{ac - b^2}} \right] \right\}, \end{aligned} \quad (2.87)$$

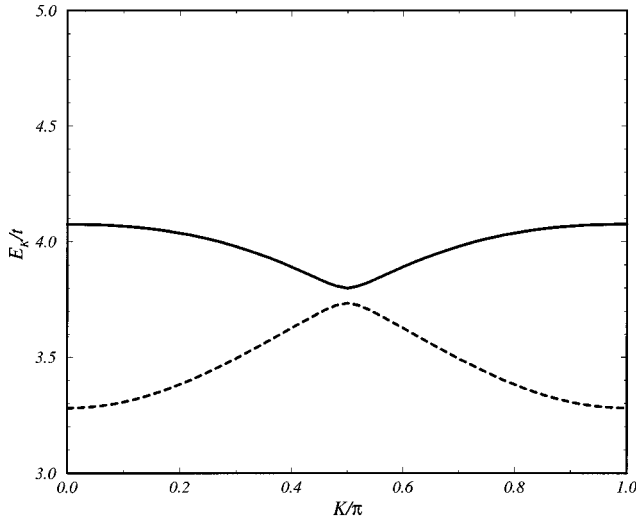


FIG. 2. Energy of excitons as a function of center-of-mass momentum K with $U=5t$, $V=2t$, and $\delta=0.2$.

where

$$a = x + 3J + 5\delta^2 J + J(1 - \delta^2)\cos 2K, \quad (2.88)$$

$$b = J(1 - \delta^2)\sin 2K, \quad (2.89)$$

$$c = x + J(1 - \delta^2) - J(1 - \delta^2)\cos 2K. \quad (2.90)$$

By solving the equations

$$1 + G(0; E_K)V + |G(2; E_K)|V = 0, \quad (2.91)$$

$$1 + G(0; E_K)V - |G(2; E_K)|V = 0, \quad (2.92)$$

we can compute the energy of the moving excitons. In Fig. 2, we have described the energy of the excitons as a function of the center-of-mass momentum K . There are two branches in the energy spectra. The energy difference between these two branches becomes smaller when K increases, and reaches a minimum at $K = \pi/2$. The bandwidths of these two branches are approximately J .

When $V \gg J$, our results show that both A_g and B_u excitons have binding energy V , which is consistent with physical intuition.²⁸ In the strong coupling limit $U \gg V \gg t$, Guo *et al.* used a local (zero hopping limit) picture and argued, since the ground state has all sites singly occupied and the exciton states are linear combinations of configuration $\dots 11120111 \dots$, where the numbers denote site occupancies, that the exciton energy is $U - V$. The electron-hole continuum consists of all states in which the double occupancy (electron) and the empty site (hole) are separated by more than one site (e.g., $\dots 11211..1011 \dots$), which has an energy U . Thus the binding energy is V . Another prediction from our theory is that the $2A_g$ state has a lower energy than the $1B_u$, which is the observed ordering in many non-luminescent conjugated polymers.^{40,53,54} The strong Coulomb interaction regime we consider here is the reason for this ordering in our model.

D. Optical absorption

We will calculate the optical absorption from Fermi's golden rule

$$\alpha(\omega) \propto \frac{1}{\omega} \sum_n | \langle n | \mathbf{J} | g \rangle |^2 \delta(\omega - E_n), \quad (2.93)$$

where \mathbf{J} is the current operator and $|n\rangle$ is the excited state with one electron-hole pair. This expression can be written in a more general form if we denote $|v\rangle = \mathbf{J}|g\rangle$,

$$\alpha(\omega) \propto -\frac{1}{\pi\omega} \lim_{\varepsilon \rightarrow 0^+} \text{Im} \left\langle v \left| \frac{1}{\omega + i\varepsilon - H} \right| v \right\rangle. \quad (2.94)$$

Hamiltonian H referred to here is that determining the energy of the electron-hole pair with $K=0$. The current operator in the polymers reads

$$\mathbf{J} = it \sum_{l\sigma} [1 - (-1)^l \delta] (c_{l+1\sigma}^\dagger c_{l\sigma} - c_{l\sigma}^\dagger c_{l+1\sigma}). \quad (2.95)$$

Using the spinless fermions η_l and γ_l defined in Sec. II A, we rewrite Eq. (2.95) as

$$\mathbf{J} = -it\delta \sum_l (\eta_{l+1}\gamma_l - \gamma_l^\dagger \eta_{l+1}^\dagger + \eta_l\gamma_{l+1} - \gamma_{l+1}^\dagger \eta_l^\dagger). \quad (2.96)$$

Thus the optical absorption can be expressed by the electron-hole Green's function

$$\alpha(\omega) \propto -\frac{t^2\delta^2}{\pi\omega} \text{Im}[\tilde{G}(0; \omega) + \tilde{G}(2; \omega)], \quad (2.97)$$

where $\tilde{G}(l; \omega)$ is the Green's function of H , satisfying

$$\tilde{G}(z) = \mathcal{G}(z) + \mathcal{G}(z)\mathcal{T}(z)\mathcal{G}(z). \quad (2.98)$$

If we denote $G(n; \omega) = G_n$, then

$$\alpha(\omega) \propto -\frac{t^2\delta^2}{\pi\omega} \text{Im} \left\{ (G_0 + G_{-2}) - \frac{V}{D(\omega)} \right. \\ \left. \times [(G_0 + G_2)^2 + V(G_0^3 - G_0G_2^2 + G_0^2G_2 - G_2^3)] \right\} \quad (2.99)$$

and $D(\omega) = [1 + (G_0 - G_2)V][1 + (G_0 + G_2)V]$.

From Fig. 3, the B_u exciton has acquired 52% oscillator strength when $U=5t$ and $V=t$. If we increase V and thus have an exciton with a larger binding energy, the B_u exciton will gain more oscillator strength. For $U=5t$ and $V=2t$, the B_u exciton has achieved 95% strength, and the strength of the transition to the continuum is correspondingly diminished, as shown in Fig. 4. The large transition strength for the exciton state is a characteristic feature of one dimension.

III. IMPURITIES AND THE COHERENT MOTION OF EXCITON

As stated in the introduction, "pristine" samples of a polymer cannot eliminate all impurities and defects. Moreover, the fluctuations (both quantum and thermal) of the lat-

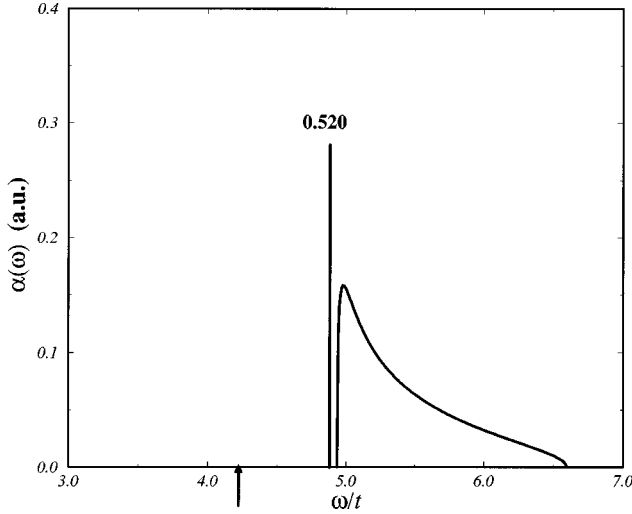


FIG. 3. Optical absorption spectrum with $U=5t$ and $V=t$. The B_u exciton occupies 0.520 of the total oscillator strength. The arrow indicates the energy of the corresponding A_g exciton.

tice are also a kind of intrinsic disorder for the electronic states in polymers.⁵⁵ Excitons represent a coherent composite particle motion of correlated electrons and holes, whereas impurities tend to produce a localized wave function. We know that an impurity has a strong effect on transport properties in many systems, especially low-dimensional materials, so a natural question arises: how do the impurities affect the coherent motion of the exciton?

In polymers, two kinds of impurity are often referred to in the literature.⁵⁶ A site impurity is represented by a local potential at site 0:

$$H_1 = V_0 \sum_{\sigma} c_{0\sigma}^{\dagger} c_{0\sigma}, \quad (3.1)$$

and a bond impurity which acts on the bond between sites 0 and 1,

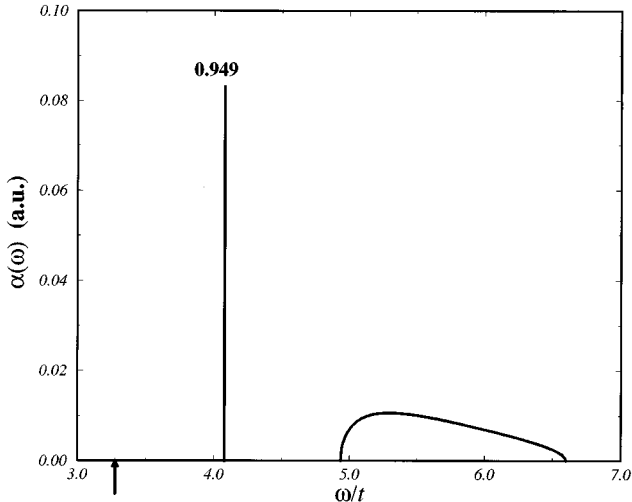


FIG. 4. Optical absorption spectrum with $U=5t$ and $V=2t$. The arrow indicates the position of the A_g exciton, and the B_u exciton takes 0.949 of the total transition strength.

$$H_2 = -W_0 \sum_{\sigma} (c_{0\sigma}^{\dagger} c_{1\sigma} + \text{H.c.}). \quad (3.2)$$

Both of these impurities have very localized (on-site) potentials. However, for a charged impurity, its potential, in principle, may be of long range. Thus we have two length scales here: one is the range of the impurity potential (l_i) and the other the range of the (screened) Coulomb interaction (l_V). The latter is equal to one lattice constant in our model. Since the impurity competes with the Coulomb interaction (in exciton states) differently in the two regimes ($l_V > l_i$ or $l_V < l_i$), impurity effects are expected to be different.

A. On-site impurity potentials

For the site and bond impurities described above, we can rewrite them in the spinless fermion representation, giving

$$H_1 = V_0 (-\eta_0^{\dagger} \eta_0 + \gamma_0^{\dagger} \gamma_0), \quad (3.3)$$

$$H_2 = -W_0 (-\eta_0 \gamma_1 - \gamma_1^{\dagger} \eta_0^{\dagger} + \gamma_0^{\dagger} \eta_1^{\dagger} + \eta_1 \gamma_0). \quad (3.4)$$

Since H_2 involves the creation and annihilation of an electron-hole pair, it must be less important than H_1 by an order of $1/U$. This can be seen more clearly by using the unitary transformation $H^S = e^{-S} H e^S$,

$$H_2^S = \frac{W_0^2}{U + 2J(1 - \delta^2)} (-\eta_0^{\dagger} \eta_0 - \eta_1^{\dagger} \eta_1 - \gamma_0^{\dagger} \gamma_0 - \gamma_1^{\dagger} \gamma_1). \quad (3.5)$$

Although the site impurity seems more realistic from the above analysis, we will study three kinds of impurity to arrive at a unified picture of impurity effects:

$$H_1^{\text{imp}} = V_0 (-\eta_0^{\dagger} \eta_0 + \gamma_0^{\dagger} \gamma_0), \quad (3.6)$$

$$H_2^{\text{imp}} = V_0 (-\eta_0^{\dagger} \eta_0 - \gamma_0^{\dagger} \gamma_0), \quad (3.7)$$

$$H_3^{\text{imp}} = V_0 (\eta_0^{\dagger} \eta_0 + \gamma_0^{\dagger} \gamma_0). \quad (3.8)$$

Hamiltonian H_1^{imp} , in which the impurity attracts the hole and repels the electron, or vice versa, imitates a local charged impurity. Hamiltonian H_2^{imp} , in which the impurity attracts both the electron and hole, acts as a trap for particles. In Hamiltonian H_3^{imp} , the impurity potentials are repulsive for both the electron and hole, describing a barrier effect. The last two types of impurity can be viewed as simulating the cross-linking and conjugation breaking effects in conjugated polymers.

There is no translation invariance once the impurity is included, so we will work in real space and the Hamiltonian we must study reads

$$\begin{aligned} H_i = & \sum_l \left\{ J(1 + \delta^2) \eta_l^{\dagger} \eta_l + \frac{1}{2} J(1 - \delta^2) (\eta_l^{\dagger} \eta_{l+2} + \eta_{l+2}^{\dagger} \eta_l) \right. \\ & + [U + J(1 - 3\delta^2)] \gamma_l^{\dagger} \gamma_l + \frac{1}{2} J(1 - \delta^2) (\gamma_l^{\dagger} \gamma_{l+2} \\ & + \gamma_{l+2}^{\dagger} \gamma_l) \left. \right\} + V \sum_l (\eta_{l+1}^{\dagger} \eta_l^{\dagger} \eta_l \eta_{l+1} + \gamma_{l+1}^{\dagger} \gamma_l^{\dagger} \gamma_l \gamma_{l+1} \\ & - \eta_{l+1}^{\dagger} \gamma_l^{\dagger} \gamma_l \eta_{l+1} - \gamma_{l+1}^{\dagger} \eta_l^{\dagger} \eta_l \gamma_{l+1}) + H_i^{\text{imp}}. \quad (3.9) \end{aligned}$$

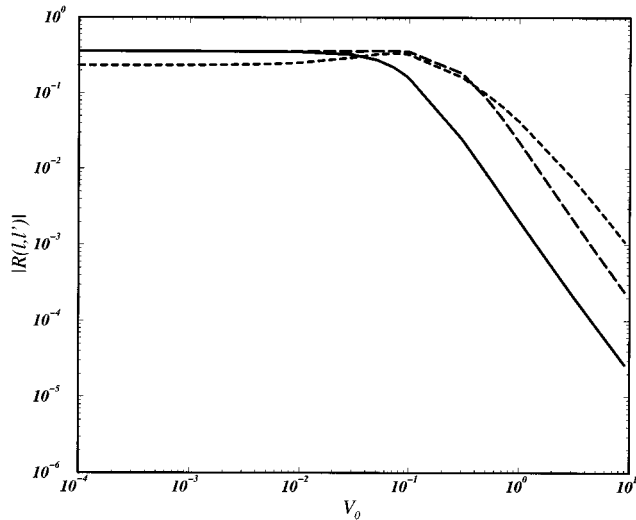


FIG. 5. Electron-hole correlation function as a function of the impurity strength V_0 for impurity potential H_1^{imp} with $U=10t$ and $V=t$. The impurity is situated at site 5 in a $N=10$ site chain. The solid, long dashed, and short dashed lines correspond to $\mathcal{R}(5,6)$, $\mathcal{R}(7,8)$, and $\mathcal{R}(3,6)$, respectively.

The key issue here is how to measure the coherence in the excitonic composite particle. We can do this by defining the correlation function between the electron and hole in the lowest state in the one electron and one hole subspace:

$$\mathcal{R}(l, l') = \frac{\langle \delta\rho_h(l) \delta\rho_e(l') \rangle}{\sqrt{\langle (\delta\rho_h(l))^2 \rangle \langle (\delta\rho_e(l'))^2 \rangle}}, \quad (3.10)$$

where the deviations are

$$\delta A = A - \langle A \rangle, \quad (3.11)$$

and the density operators of electron and hole are

$$\rho_h(l) = \eta_l^\dagger \eta_l, \quad (3.12)$$

$$\rho_e(l) = \gamma_l^\dagger \gamma_l. \quad (3.13)$$

In the impurity-free system, this correlation function (3.10) is connected with the relative wave function of the lowest exciton state $|\Psi_0\rangle = (1/\sqrt{N}) \sum_s B_s \gamma_{l+s}^\dagger \eta_l^\dagger |g\rangle$ by

$$\mathcal{R}^{\text{free}}(l, l') = |B_{l-l'}|^2. \quad (3.14)$$

When we add an impurity, the correlation is expected to decrease. The closer \mathcal{R} is to $\mathcal{R}^{\text{free}}$, the more correlated are the electron and hole in the lowest excitonic states, while \mathcal{R} approaching zero means that there is no correlation between the electron and hole; in other words, this excitonic state has lost all its coherence.

The effects of the first kind of impurity are illustrated in Fig. 5, which shows the electron-hole correlation functions for different sites in a finite system of size $N=10$. We emphasize that the parameters we use ($U=10t$ and $V=t$) ensure that the exciton has a very localized *relative* wave function, so that finite system corrections and the boundary condition effects are not important. In Fig. 5, all the correlation functions exhibit a crossover behavior around $V_0 \sim 0.1t$. This can be understood in term of a relevant en-

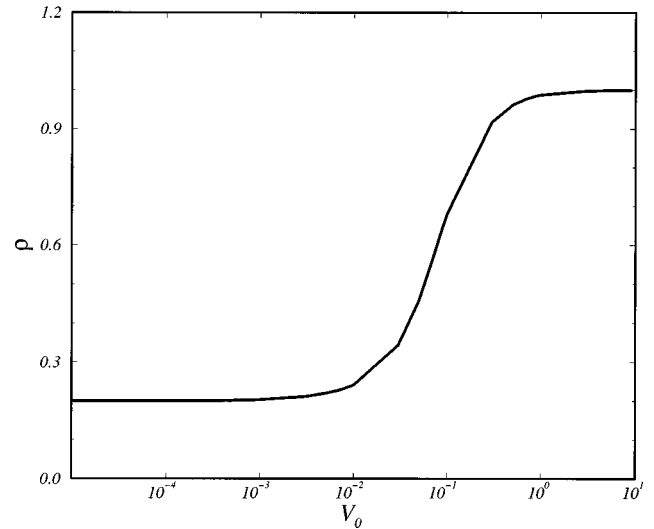


FIG. 6. The hole density at the impurity site vs impurity strength V_0 for the impurity potential H_1^{imp} . The parameters here are the same as in Fig. 5.

ergy scale of the exciton, namely, the width of the exciton band, which equals $J=2t^2/U$. This crossover behavior, which occurs at $V_0 \sim J$, describes the localization of the exciton, i.e., the free exciton becomes trapped. We can also calculate the charge density at the impurity site as the impurity strength increases. Since in an impurity-free system the hole (electron) is uniformly distributed, and from our exciton theory the electron and hole do not tend to occupy the same site, the hole density at the impurity site is $2/N$. We see a crossover again in Fig. 6 when V_0 is comparable to the bandwidth J . After this crossover, the hole density at the impurity site approaches 1, clearly showing that the exciton is trapped by the impurity, and the correlation between the electron and hole gradually vanishes, although, as indicated in Fig. 7, they are bound together near the impurity.

For the second type of impurity, from Fig. 8, a crossover is also observed if the impurity strength is similar to the

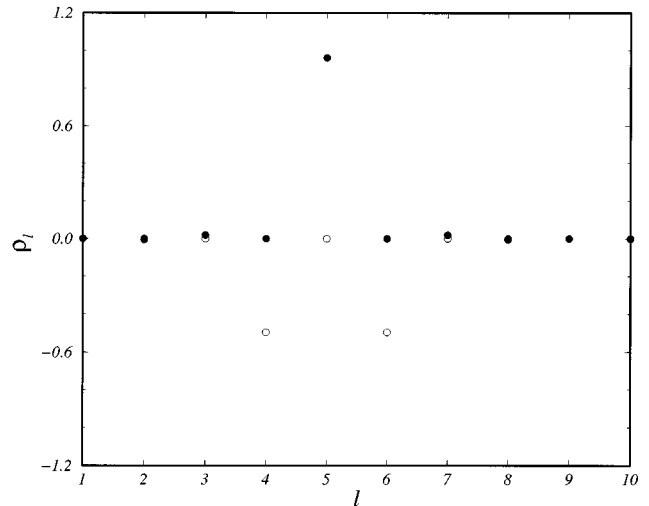


FIG. 7. Distribution of charge density in real space for the first type of impurity, H_1^{imp} . The solid circles describe the hole density, while the open ones are for the electron density. Here $U=10t$, $V=t$, and $V_0=0.5t$.

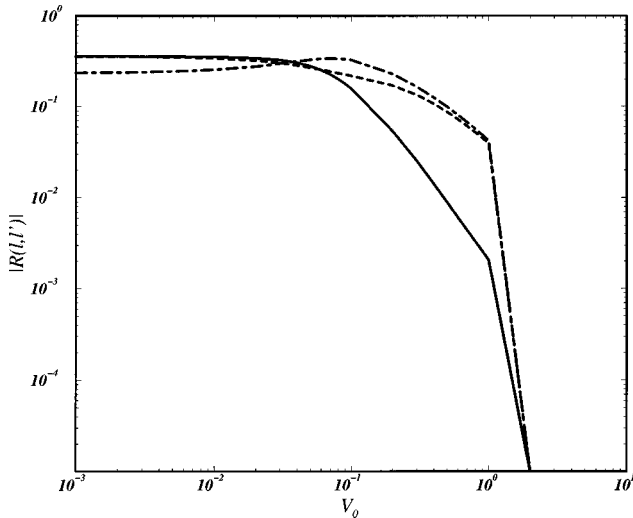


FIG. 8. Electron-hole correlation function, as a function of the impurity strength V_0 for the impurity potential H_2^{imp} with $U=10t$ and $V=t$. The impurity is located at site 5 in a $N=10$ chain. The solid, dashed, and dot-dashed lines illustrate $\mathcal{R}(5,6)$, $\mathcal{R}(3,4)$, and $\mathcal{R}(3,6)$, respectively.

exciton bandwidth, again indicating that the exciton is trapped. But when V_0 is larger than V , the correlation function abruptly falls to zero, which implies the total breakdown of the exciton as a composite particle. This is because, when V_0 is large enough, it is a lower energy for the impurity to trap the electron and hole separately rather than the impurity trapping the hole and then the electron being trapped near the hole due to the Coulomb interaction (as for the first kind of impurity). Thus the electron and the hole occupy the same site and they have no Coulomb interaction. This is not an exciton.

Now we consider the third type of impurity. The correlation function behaviors in Fig. 9 seem more complicated

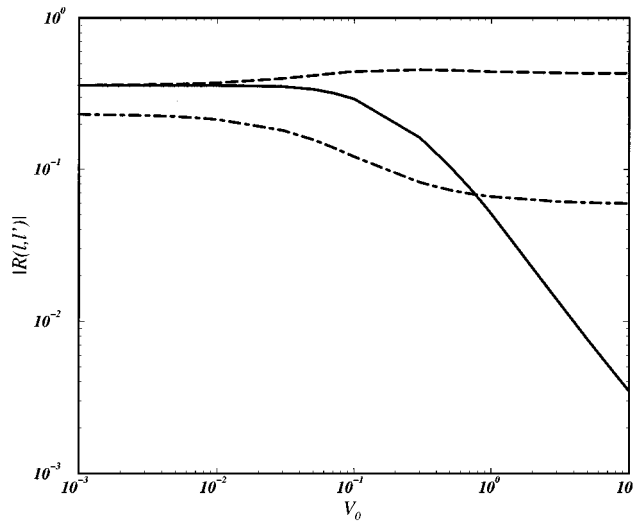


FIG. 9. Electron-hole correlation function as a function of the impurity strength V_0 for the third kind of impurity H_3^{imp} in a $N=10$ chain. Parameters are the same as for Fig. 8, $U=10t$ and $V=t$. The solid, dashed, and dot-dashed lines are for $\mathcal{R}(5,6)$, $\mathcal{R}(3,4)$, and $\mathcal{R}(3,6)$, respectively.

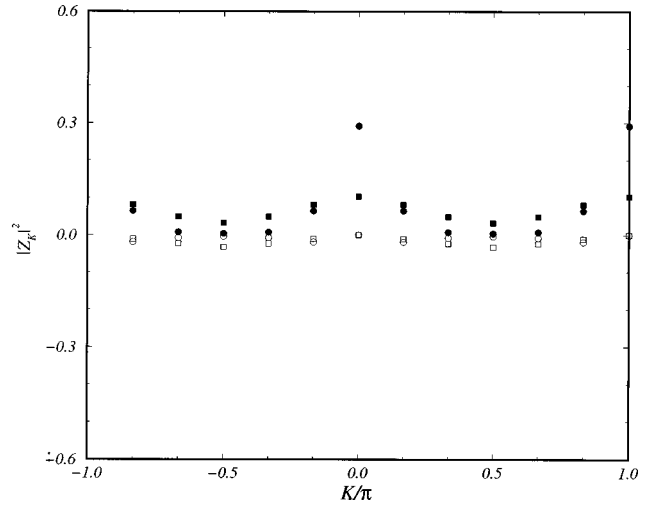


FIG. 10. Distribution $|Z_K|^2$ for the impurity potential H_1^{imp} with $U=10t$ and $V=t$ in a $N=12$ chain. There are two exciton branches (A_g and B_u). The solid symbols indicate the amplitude of excitons in the A_g branch, and the open ones give the amplitude of excitons in the B_u branch. The circle corresponds to $V_0=0.1t$, the situation before the crossover, and the box corresponds to $V_0=t$, which is larger than the crossover value.

than for the other two types of impurity. The correlation function in which the hole is at the impurity site shows an analogous crossover behavior when V_0 is near the exciton bandwidth J to the first and second types of impurity. However, if both the electron and the hole are left (or right) of the impurity, from the correlation function we see that they have not felt the impurity. On the other hand, if the electron and the hole sit on different sides of the impurity, there is a crossover at $V_0 \sim J$, but part of correlation between the electron and hole survives.

The different effects of these three kinds of impurity can be further understood if we project the lowest excitonic state to the free exciton states with momentum K . We depict in Figs. 10, 11, and 12 the distribution $|Z_K|^2$, where $Z_K = \langle \Psi_K | \Psi \rangle$, and $|\Psi\rangle$ is the lowest excitonic state in these three disordered systems. In the impurity-free system, the lowest state is the linear combination of exciton states with $K=0$ and $K=\pi$ (they are degenerate). In the presence of an impurity, the exciton state will be scattered to other exciton states with different K and the distribution of momenta will broaden from the δ function. A free exciton state with a specific K can be defined only when the width of the distribution of momentum is narrow enough (i.e., the lifetime of this state is long enough). This is analogous to the quasiparticle in Landau's Fermi liquid theory.⁵⁷ From these figures, we see that for the first and second types of impurities, after the crossover at $V_0 \sim J$ the distribution in momentum space becomes so broad that we can hardly identify the original exciton state with momentum $K=0$ or $K=\pi$. For the second type of impurity, when V_0 is larger than V , the final state has no distribution at all on any free exciton state, also indicating that the final state is no longer excitonic. However, for the third kind of impurity, after the crossover at $V_0 \sim J$, the distribution in momentum space still has two sharp peaks at $K=0$ and $K=\pi$. This is the reason why the exciton is still

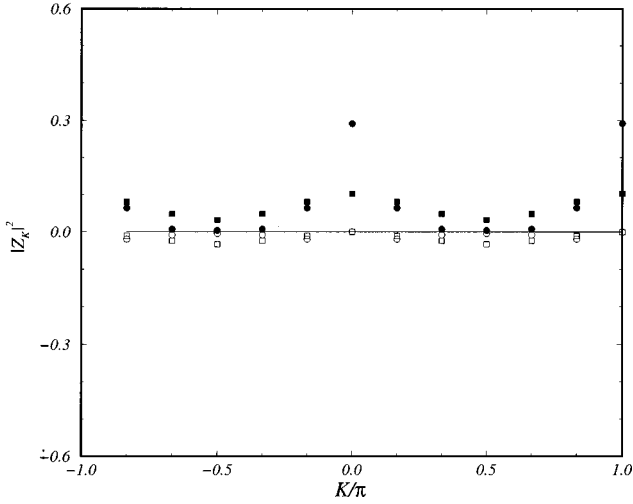


FIG. 11. Distribution $|Z_K|^2$ for the second kind of impurity potential H_2^{imp} with $U=10t$ and $V=t$ in a $N=12$ chain. The solid and open symbols have the same meanings as in Fig. 10. The circle describes the case of $V_0=0.1t$ and the box describes $V_0=t$. The line is for the case $V_0=2t$. The vanishing amplitude in every excitation state shows the breakdown of the exciton.

coherent, as shown in the correlation functions, and in this sense the exciton can be regarded as a quasiparticle in this disordered system.

B. Extended impurity potentials

For a charged impurity, the range of the (screened Coulomb) potential can be extended over several lattice constants. As an illustration, here we consider a specific impurity potential,

$$H_4^{\text{imp}} = V_0(-\eta_0^\dagger \eta_0 + \gamma_0^\dagger \gamma_0) + \frac{V_0}{2}(-\eta_1^\dagger \eta_1 + \gamma_1^\dagger \gamma_1 - \eta_{-1}^\dagger \eta_{-1} + \gamma_{-1}^\dagger \gamma_{-1}). \quad (3.15)$$

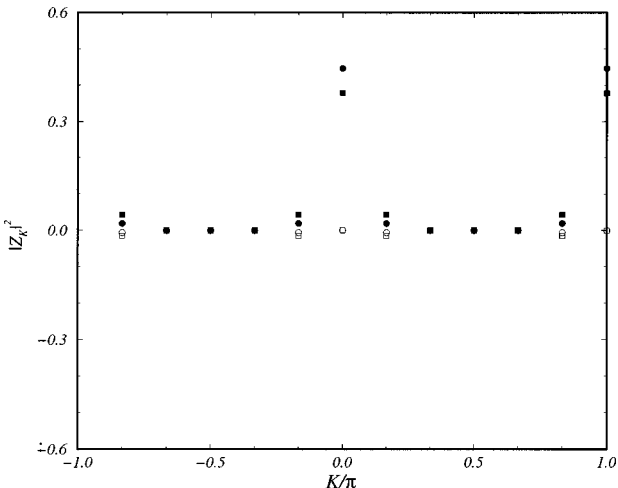


FIG. 12. Distribution $|Z_K|^2$ for the third kind of impurity H_3^{imp} with $U=10t$ and $V=t$ in a $N=12$ chain. The circle and box correspond to $V_0=0.1t$ and $V_0=t$, respectively.

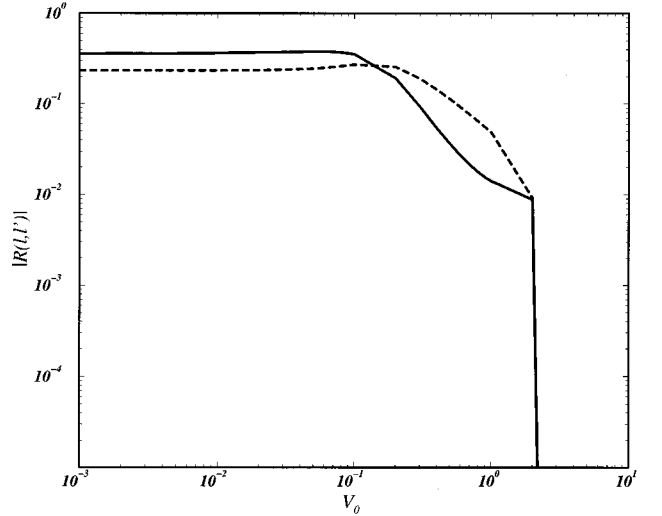


FIG. 13. Electron-hole correlation function as a function of the impurity strength V_0 for a charged impurity H_4^{imp} in a $N=10$ chain. Parameters are the same as for Fig. 8, $U=10t$ and $V=t$. The solid and dashed lines are for $\mathcal{R}(5,6)$ and $\mathcal{R}(3,6)$, respectively.

Its range (l_i) is three lattice constants which is longer than that of the Coulomb interaction (l_V). The correlation functions are illustrated in Fig. 13, from which we observe again a crossover around $V_0 \sim J$, indicating the free exciton becomes trapped. Interestingly, when V_0 is sufficiently large compared to V , the correlation function falls further abruptly to zero, indicating the dissociation of the exciton into an uncorrelated electron-hole pair. Note that this does not occur for the charged impurity H_1^{imp} with the on-site potential, since the impurity range is then less than the trapped exciton size. From charge densities shown in Fig. 14, we find that for $V_0=0.5t$ (just after the first crossover), both the electron and the hole (thus the exciton) are trapped around the impurity. For $V_0=5t$ (after the correlation goes to zero), the hole is trapped by the impurity while the elec-

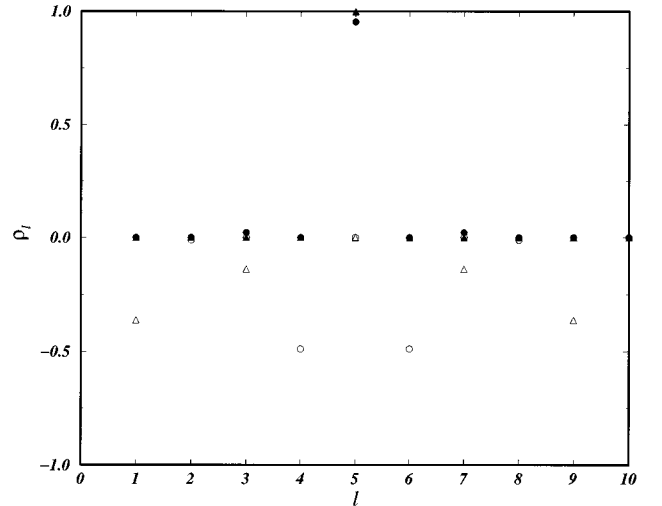


FIG. 14. Distribution of charge density in real space for a charged impurity with extended potential H_4^{imp} . The solid symbols describe the hole density and the open ones are for the electron density. The circles and triangles correspond to $V_0=0.5t$ and $V_0=5t$, respectively. Here $U=10t$, $V=t$.

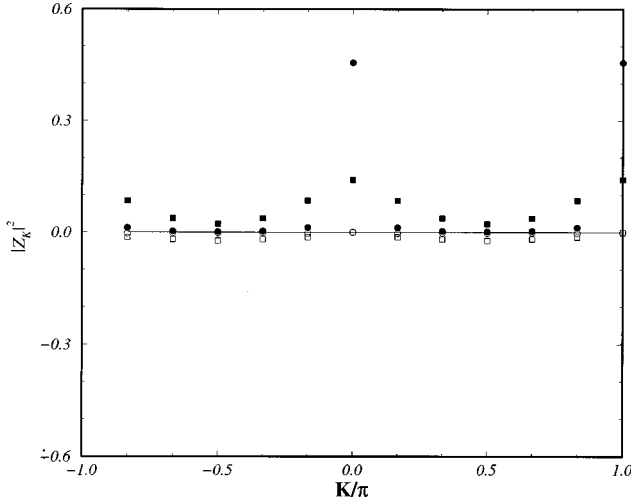


FIG. 15. Distribution $|Z_K|^2$ for a charged impurity with extended potential H_4^{imp} for $U=10t$ and $V=t$ in a $N=12$ chain. The solid and open symbols have the same meaning as in Fig. 10. The circle describes the $V_0=0.1t$ case, the box describes $V_0=t$, and the line is for $V_0=5t$. The vanishing amplitude in every exciton state indicates the dissociation of the exciton.

tron is repelled from the impurity. The dissociation of excitons here is easily understood. Because the impurity attracts the hole and repels the electron, when the impurity strength becomes sufficiently strong, the Coulomb attraction cannot overcome the impurity repulsion to bind the electron and hole together. This impurity-induced exciton dissociation may be invoked to interpret impurity-enhanced photoconductivity observed in certain experiments. We can project the lowest excitonic state in the system with the impurity to free exciton states with different momenta. In Fig. 15, the distribution in momentum space changes from a sharply localized one ($V_0=0.1t$, before the crossover) to a very broad Gaussian distribution ($V_0=0.5t$, after the crossover) and finally goes to zero ($V_0=5t$). This is consistent with the picture that the free exciton becomes trapped, then dissociates into an uncorrelated electron-hole pair with increasing impurity strength.

IV. INTERCHAIN COUPLING AND INTERCHAIN EXCITONS

The interchain coupling can strongly influence the energy and stability of the nonlinear excitations such as solitons and polarons. Current interest in interchain coupling and the intrachain and interchain exciton crossover in polymers stems from the experimentally observed large amount of interchain excitations in luminescent polymers like PPV. However, the concept of an interchain exciton and how to distinguish the interchain and intrachain excitons, are not very clear. The wave function is not so useful to specify whether a state is an interchain or intrachain exciton, because the wave function of any state, in principle, will spread over the whole system if interchain coupling is present.

To demonstrate interchain exciton states in our approach, we study a two-chain system coupled by the nearest-neighbor hopping,

$$H_{\text{hop}} = -t_{\perp} \sum_{l\sigma} (c_{1l\sigma}^{\dagger} c_{2l\sigma} + \text{H.c.}), \quad (4.1)$$

and nearest-neighbor interchain Coulomb interaction,

$$H_{\text{Cou}} = V_{\perp} \sum_l (\rho_{1l} - 1)(\rho_{2l} - 1). \quad (4.2)$$

Here 1,2 are chain indices. Now the unperturbed Hamiltonian in the large- U limit becomes

$$\begin{aligned} \tilde{H}_0 = H'_0 + H_{\text{hop}} = & \sum_{i,k} (\epsilon_k \eta_{ik}^{\dagger} \eta_{ik} + \tilde{\epsilon}_k \gamma_{ik}^{\dagger} \gamma_{ik}) \\ & + t_{\perp} \sum_l (\eta_{2l}^{\dagger} \eta_{1l} - \gamma_{1l}^{\dagger} \gamma_{2l} + \text{H.c.}). \end{aligned} \quad (4.3)$$

In momentum space, this is

$$\begin{aligned} \tilde{H}_0 = & \sum_{i,k} (\epsilon_k \eta_{ik}^{\dagger} \eta_{ik} + \tilde{\epsilon}_k \gamma_{ik}^{\dagger} \gamma_{ik}) \\ & + t_{\perp} \sum_k (\eta_{2k}^{\dagger} \eta_{1k} - \gamma_{1k}^{\dagger} \gamma_{2k} + \text{H.c.}), \end{aligned} \quad (4.4)$$

which can be readily diagonalized, yielding

$$\tilde{H}_0 = \sum_{I,k} (E_k^I \tilde{\eta}_{Ik}^{\dagger} \tilde{\eta}_{Ik} + \tilde{E}_k^I \tilde{\gamma}_{Ik}^{\dagger} \tilde{\gamma}_{Ik}). \quad (4.5)$$

Here $I=1,2$ is the band index (hereafter we use small i,j for the chain indices, and capital I,J for the band indices). The details of the diagonalization are given in Appendix B. Now we have two conduction and two valence bands with the dispersion relations

$$E_k^{1,2} = \epsilon_k \mp t_{\perp}, \quad (4.6)$$

$$\tilde{E}_k^{1,2} = \tilde{\epsilon}_k \mp t_{\perp}. \quad (4.7)$$

The interaction Hamiltonian now contains two parts

$$H_V = H_{\text{int}} + H_{\text{Cou}}. \quad (4.8)$$

The electron-hole interaction part of H_V , which is relevant to the exciton state, is

$$\begin{aligned} H_V^{e-h} = & -V \sum_{i,l} (\eta_{il+1}^{\dagger} \gamma_{il}^{\dagger} \gamma_{il} \eta_{il+1} + \gamma_{il+1}^{\dagger} \eta_{il}^{\dagger} \eta_{il} \gamma_{il+1}) \\ & - V_{\perp} \sum_l (\eta_{1l}^{\dagger} \gamma_{2l}^{\dagger} \gamma_{2l} \eta_{1l} + \gamma_{1l}^{\dagger} \eta_{2l}^{\dagger} \eta_{2l} \gamma_{1l}). \end{aligned} \quad (4.9)$$

If we define local fermion operators

$$\tilde{\eta}_{Il} = \frac{1}{\sqrt{N}} \sum_k e^{ikl} \tilde{\eta}_{Ik}, \quad (4.10)$$

$$\tilde{\gamma}_{Il} = \frac{1}{\sqrt{N}} \sum_k e^{ikl} \tilde{\gamma}_{Ik}, \quad (4.11)$$

we can rewrite Eq. (4.9) as

$$\begin{aligned}
H_V^{e-h} = & -\frac{V}{2} \sum_{IJ} \sum_I (\tilde{\eta}_{I+1}^\dagger \tilde{\gamma}_{JI}^\dagger \tilde{\gamma}_{JI} \tilde{\eta}_{I+1} \\
& + \tilde{\gamma}_{I+1}^\dagger \tilde{\eta}_{JI}^\dagger \tilde{\eta}_{JI} \tilde{\gamma}_{I+1}) \\
& + \frac{V}{2} \sum_I (\tilde{\eta}_{1I+1}^\dagger \tilde{\gamma}_{1I}^\dagger \tilde{\gamma}_{2I} \tilde{\eta}_{2I+1} + \tilde{\eta}_{1I+1}^\dagger \tilde{\gamma}_{2I}^\dagger \tilde{\gamma}_{1I} \tilde{\eta}_{2I+1} \\
& + \tilde{\gamma}_{1I+1}^\dagger \tilde{\eta}_{1I}^\dagger \tilde{\eta}_{2I} \tilde{\gamma}_{2I+1} + \tilde{\gamma}_{1I+1}^\dagger \tilde{\eta}_{2I}^\dagger \tilde{\eta}_{1I} \tilde{\gamma}_{2I+1} + 1 \Leftrightarrow 2) \\
& - \frac{V_\perp}{2} \sum_{IJ} \sum_I \tilde{\gamma}_{II}^\dagger \tilde{\eta}_{JI}^\dagger \tilde{\eta}_{JI} \tilde{\gamma}_{II} \\
& - \frac{V_\perp}{2} \sum_I (\tilde{\eta}_{1I}^\dagger \tilde{\gamma}_{1I}^\dagger \tilde{\gamma}_{2I} \tilde{\eta}_{2I} + \tilde{\eta}_{1I}^\dagger \tilde{\gamma}_{2I}^\dagger \tilde{\gamma}_{1I} \tilde{\eta}_{2I} + 1 \Leftrightarrow 2).
\end{aligned} \tag{4.12}$$

Thus we can construct the exciton wave function in this two-chain system as

$$|\Psi_K\rangle = \sum_{IJ} \sum_s B_{s,K}^{IJ} |\psi_{s,K}^{IJ}\rangle. \tag{4.13}$$

Here the center-of-mass momentum K is still a good quantum number, and the basis is

$$|\psi_{s,K}^{IJ}\rangle = \frac{1}{\sqrt{N}} \sum_I e^{iKI} \tilde{\gamma}_{II+s}^\dagger \tilde{\eta}_{JI}^\dagger |g\rangle, \tag{4.14}$$

which means the exciton state is a combination of every possible electron-hole excitation in different conduction and valence bands. The free electron-hole pair Green's function under the basis Eq. (4.14) is

$$\left\langle \psi_{r,K}^{I'J'} \left| \frac{1}{z_K - \tilde{H}_0} \right| \psi_{s,K}^{IJ} \right\rangle = \delta_{I'I} \delta_{J'J} G^{IJ}(r-s; z_K), \tag{4.15}$$

$$G^{IJ}(l; z_K) = \frac{1}{N} \sum_k \frac{e^{ikl}}{z_K - (\tilde{E}_k^I + E_{-k+K}^J)}, \tag{4.16}$$

and the scattering potential is written as

$$\langle \psi_{s,K}^{I'J'} | H_V^{e-h} | \psi_{s',K}^{IJ} \rangle = \delta_{ss'} \left(-\frac{V}{2} \delta_{s1} - \frac{V}{2} \delta_{s-1} - \frac{V_\perp}{2} \delta_{s0} \right) F(I', J'; I, J), \tag{4.17}$$

with $F(I, J; I, J) = 1$ and $F(1, 1; 2, 2) = F(2, 2; 1, 1) = F(1, 2; 2, 1) = F(2, 1; 1, 2) = 1$, and otherwise $F = 0$. We can solve for the exciton states by locating the roots of the determinant $\det(1 - \mathcal{G}\mathcal{U})$ according to t matrix theory. The whole determinant can be decomposed into blocks by appropriate transformations and we achieve two subdeterminants,

$$D_1 = \begin{vmatrix} 1 + \frac{V_\perp}{2} G^{11}(0; z_K) & \frac{V_\perp}{2} G^{11}(0; z_K) \\ \frac{V_\perp}{2} G^{22}(0; z_K) & 1 + \frac{V_\perp}{2} G^{22}(0; z_K) \end{vmatrix} \tag{4.18}$$

and

$$D_2 = \begin{vmatrix} 1 + \frac{V_\perp}{2} G^{12}(0; z_K) & \frac{V_\perp}{2} G^{12}(0; z_K) \\ \frac{V_\perp}{2} G^{21}(0; z_K) & 1 + \frac{V_\perp}{2} G^{21}(0; z_K) \end{vmatrix}. \tag{4.19}$$

D_1 and D_2 are determined only by interchain Coulomb interaction V_\perp corresponding to *interchain* excitons, and two subdeterminants,

$$D_3 = \begin{vmatrix} 1 + \frac{V}{2} [G^{11}(0; z_K) + G^{22}(0; z_K)] & \frac{V}{2} [G^{11}(-2; z_K) + G^{22}(-2; z_K)] \\ \frac{V}{2} [G^{11}(2; z_K) + G^{22}(2; z_K)] & 1 + \frac{V}{2} [G^{11}(0; z_K) + G^{22}(0; z_K)] \end{vmatrix} \tag{4.20}$$

and

$$D_4 = \begin{vmatrix} 1 + \frac{V}{2} [G^{12}(0; z_K) + G^{21}(0; z_K)] & \frac{V}{2} [G^{12}(-2; z_K) + G^{21}(-2; z_K)] \\ \frac{V}{2} [G^{12}(2; z_K) + G^{21}(2; z_K)] & 1 + \frac{V}{2} [G^{12}(0; z_K) + G^{21}(0; z_K)] \end{vmatrix}, \tag{4.21}$$

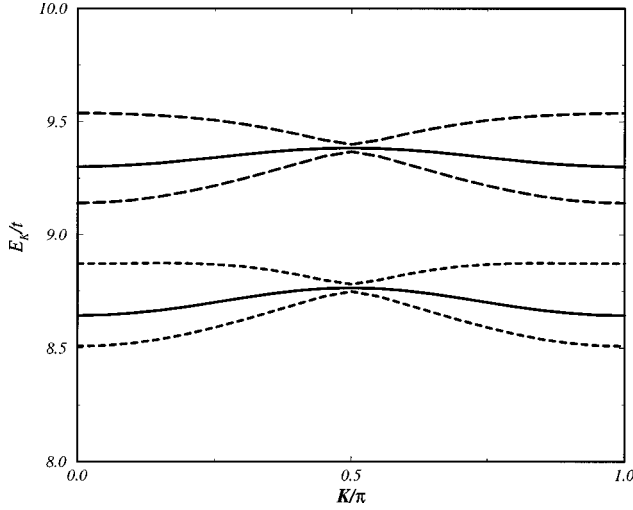


FIG. 16. Intrachain and interchain exciton bands with $U=10t$, $V=t$, $t_{\perp}=0.5t$, and $V_{\perp}=t$. The two solid lines describe the dispersion of the interchain exciton, and the four dashed lines are for intrachain excitons.

which are determined only by the intrachain Coulomb interaction V corresponding to *intrachain* excitons. Equations $D_1=0$ and $D_2=0$ have a single root, respectively, whereas both $D_3=0$ and $D_4=0$ have two roots. Thus there are a total of six exciton bands: two interchain exciton bands and four intrachain exciton bands. Figures 16 and 17 show these intrachain and interchain exciton bands. The relative energy ordering of the interchain and intrachain excitons depends on the ratio V_{\perp}/V .

It is interesting to study the wave function of the interchain excitons. The static interchain exciton can be represented in real space as

$$|\Psi_{K=0}\rangle = \sum_{ij} \sum_s A_s^{ij} \frac{1}{\sqrt{N}} \sum_l \gamma_{il+s}^{\dagger} \eta_{jl}^{\dagger} |g\rangle. \quad (4.22)$$

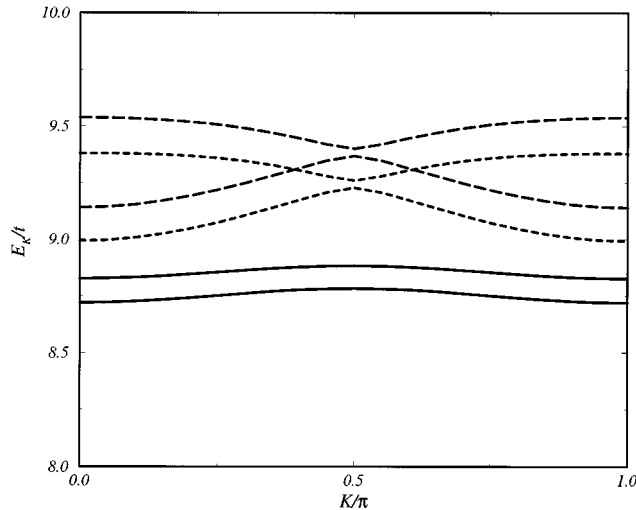


FIG. 17. Intrachain and interchain exciton bands with $U=10t$, $V=t$, $t_{\perp}=0.2t$, and $V_{\perp}=1.5t$. Solid lines are the energy spectra for interchain excitons. Here the interchain exciton is the lowest excited state.

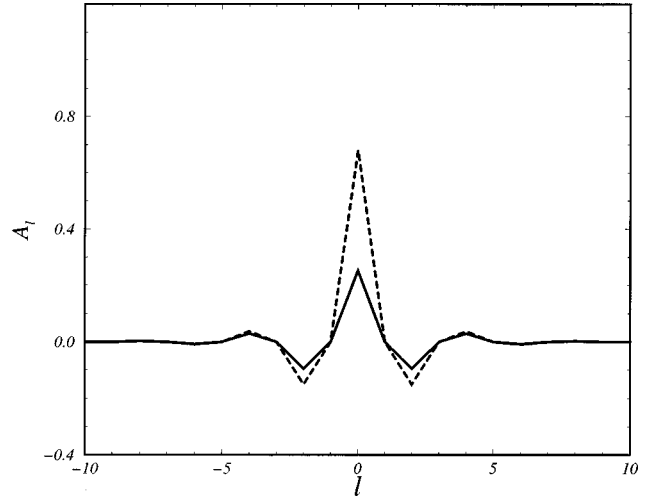


FIG. 18. Wave functions of the lower static interchain exciton with $U=10t$, $V=t$, $t_{\perp}=0.2t$, and $V_{\perp}=t$. The solid line gives the relative amplitude that the electron and hole are in the same chain, and the dashed line gives the amplitude that they are in different chains.

For the lower exciton state determined by $D_1(z_0)=0$, we obtain

$$A_s^{11} = -A_s^{22} = -\frac{G^{11}(s; z_0) - G^{22}(s; z_0)}{2\sqrt{-[G^{11}(0; z_0) + G^{22}(0; z_0)]'}}, \quad (4.23)$$

which represents the amplitude for the electron and hole being on the same chain; while

$$A_s^{21} = -A_s^{12} = -\frac{G^{11}(s; z_0) + G^{22}(s; z_0)}{2\sqrt{-[G^{11}(0; z_0) + G^{22}(0; z_0)]'}}, \quad (4.24)$$

is the amplitude that the electron and hole are on different chains. Here

$$G^{11}(0; z) = -\frac{1}{\sqrt{(E_G - z - 2t_{\perp})(E_G - z - 2t_{\perp} + W)}}, \quad (4.25)$$

$$G^{22}(0; z) = -\frac{1}{\sqrt{(E_G - z + 2t_{\perp})(E_G - z + 2t_{\perp} + W)}}, \quad (4.26)$$

where E_G is defined as Eq. (2.50) and $W=4J(1+\delta^2)$. Figure 18 illustrates the intrachain wave function A_s^{11} and interchain wave function A_s^{21} for this interchain exciton state. We can see that although the state is for an interchain exciton, there is still some probability for the electron and hole to be on the same chain.

For the higher interchain exciton determined by $D_2(z_0)=0$, we have

$$A_s^{11} = A_s^{22} = 0, \quad (4.27)$$

$$A_s^{21} = A_s^{12} = -\frac{G^{12}(s; z_0)}{\sqrt{-[G^{12}(0; z_0)]'}}, \quad (4.28)$$

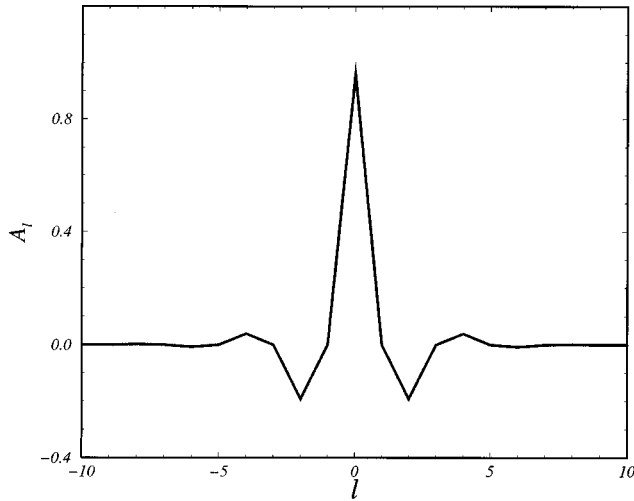


FIG. 19. Wave functions of the higher static interchain exciton with $U=10t$, $V=t$, $t_{\perp}=0.2t$, and $V_{\perp}=t$. Here the intrachain amplitude is zero.

$$G^{12}(0;z) = -\frac{1}{\sqrt{(E_G-z)(E_G-z+W)}}. \quad (4.29)$$

In this interchain exciton, there is no relative amplitude between the electron and hole if they are on the same chain. In Fig. 19, we plot the wave function A_s^{21} for this interchain exciton.

For more complicated Coulomb interactions within and between the chains, the exact interchain and intrachain exciton poles are difficult to obtain analytically. Instead, we can measure the correlation between the electron and hole using Eq. (3.10). In Fig. 20, we depict the intrachain and interchain electron-hole correlation functions for our simple interchain coupling situation for two $N=12$ chains. Here we choose a fixed interchain hopping $t_{\perp}/t=0.2$. The transition at

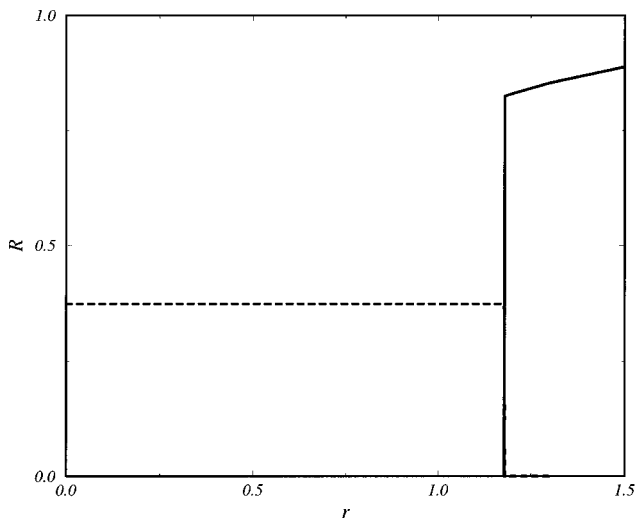


FIG. 20. Intra/interchain electron-hole correlation vs $r=V_{\perp}/V$ in a two-chain system. Each chain has $N=12$ sites and the parameters are $U=10t$, $V=t$, and $t_{\perp}=0.2t$. The intrachain correlation function illustrated here by the dashed line is $\mathcal{R}(5,6)$, and the interchain correlation function given by the solid line is $\mathcal{R}(5,17)$, where site $12+i$ indicates site i in the second chain.

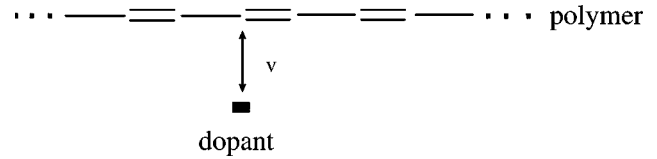


FIG. 21. Schematic diagram of the charge transfer from a polymer chain to a dopant molecule. The dopant has an acceptor level which interacts with the polymer by nearest-neighbor hopping v .

$V_{\perp}/V=1.18$ shows that the lowest exciton state changes from an intrachain exciton to an interchain one.

V. CHARGE TRANSFER IN A MOLECULARLY DOPED POLYMER

Photoinduced charge transfer from a polymer chain to an adjacent dopant molecule, such as in PPV/ C_{60} blends has attracted much recent attention, because it can greatly increase the photoconductivity in polymers. In recent theoretical work on this phenomenon, Rice and Gartstein³⁹ proposed a mechanism to explain the observed ultrafast time scale of this process. In this section, instead of discussing the time scale, we attempt to calculate the final state wave function of the whole system comprising the polymer chain and dopant molecule. This can tell us what part of the electron in the exciton has transferred from the chain to the dopant. To make our idea more transparent, let us briefly describe this photoinduced charge transfer process. In the ground state, there is no overlap between the chain and the dopant. The photoexcitation produces an exciton state in the polymer chain. Then, due to the coupling between the polymer and the dopant molecule, the electron (or hole) will transfer from the chain to the adjacent molecule. As a simplified Hamiltonian, we consider

$$H = H_{\text{chain}} + \Delta_e \sum_m c_m^{\dagger} c_m + H_{\text{tran}}. \quad (5.1)$$

Here we are modeling the dopant molecule by assuming it has an acceptor level with energy Δ_e , which couples to the polymer chain only by nearest-neighbor hopping,

$$H_{\text{tran}} = -v \sum_m (c_m^{\dagger} \gamma_0 + \text{H.c.}) = -\frac{v}{\sqrt{N_{m,k}}} \sum (c_m^{\dagger} \gamma_k + \text{H.c.}). \quad (5.2)$$

A schematic diagram of our model is shown in Fig. 21. The whole system consists of a polymer chain and N_d dilute non-interacting dopants. Before the coupling between the polymer chain and the dopant is switched on, the system has an exciton state on the polymer chain. When we turn on the coupling, the electron in the exciton will transfer between the chain and the molecule. Thus we can construct a variational wave function,

$$|\Psi\rangle = a|\Psi_0\rangle + \frac{1}{\sqrt{N_d}} \sum_m \sum_k a_k c_m^{\dagger} \gamma_k |\Psi_0\rangle, \quad (5.3)$$

with the condition $\langle\Psi|\Psi\rangle=1$. The first term describes the electron remaining on the chain as a component of the exciton and the second term describes that the electron with dif-

ferent momentum has a different probability of transferring to the dopant molecule. Here $|\Psi_0\rangle$ is the assumed static exciton state within the polymer chain,

$$|\Psi_0\rangle = \sum_s B_s \frac{1}{\sqrt{N}} \sum_l \gamma_{l+s}^\dagger \eta_l^\dagger |g\rangle, \quad (5.4)$$

which can be represented by the relative momentum between the electron and hole

$$|\Psi_0\rangle = \sum_k B_k \frac{1}{\sqrt{N}} \gamma_k^\dagger \eta_{-k}^\dagger |g\rangle. \quad (5.5)$$

Its energy is

$$\langle \Psi_0 | H_{\text{chain}} | \Psi_0 \rangle = E_0. \quad (5.6)$$

The variational state $|\Psi\rangle$ must have a lower energy than E_0 ,

$$\epsilon = \langle \Psi | H | \Psi \rangle - E_0 < 0. \quad (5.7)$$

From $(\partial\epsilon/\partial a) = 0$ and $(\partial\epsilon/\partial a_k) = 0$, we obtain two coupled equations:

$$-\sqrt{\frac{N_d}{N}} a v = a_k [\epsilon + E_0 - (\epsilon_k + \Delta_e)], \quad (5.8)$$

$$a \epsilon = \frac{1}{N} \sum_k a_k |B_k|^2 \sqrt{\frac{N_d}{N}} v. \quad (5.9)$$

Using Eq. (5.8), a_k can be eliminated from Eq. (5.9) and we have the eigenvalue equation for ϵ

$$\epsilon = c \frac{1}{N} \sum_k \frac{v^2 |B_k|^2}{\epsilon + E_0 - (\epsilon_k + \Delta_e)} \equiv c F(\epsilon). \quad (5.10)$$

Here $c \equiv N_d/N$ is the dopant concentration. Once we have found the negative solution of ϵ , the probability that the exciton remains on the chain is

$$a^2 = \frac{1}{1 - c F'(\epsilon)}, \quad (5.11)$$

where $F'(\epsilon) = [dF(\epsilon)/d\epsilon]$. So the probability of charge transfer is

$$P = 1 - a^2 = \frac{-c F'(\epsilon)}{1 - c F'(\epsilon)}. \quad (5.12)$$

For the B_u exciton in the polymer chain

$$B_k = \sum_l B_l^+ e^{-ikl}. \quad (5.13)$$

If we assume for demonstration purposes that the exciton is highly localized (this is not necessary in our theory), i.e., $B_1^+ = B_{-1}^+ = (1/\sqrt{2})$ and $B_l^+ = 0$ for other l , then

$$B_k = \sqrt{2} \cos k, \quad (5.14)$$

and we can write $F(\epsilon)$ in a very compact form:

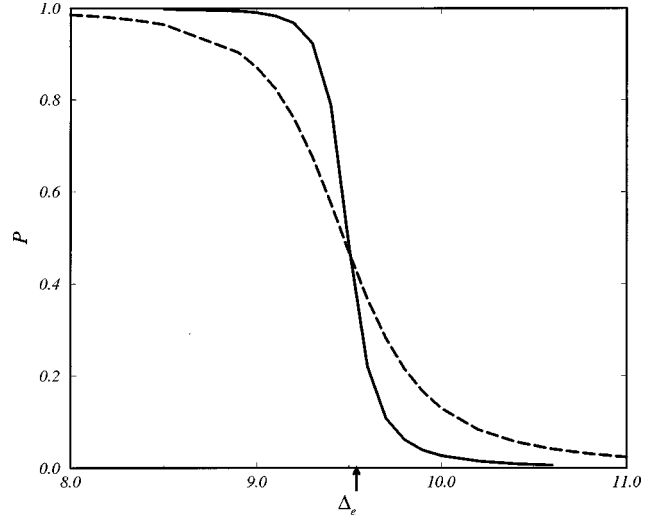


FIG. 22. Probability of charge transfer of the B_u state as a function of acceptor level Δ_e . The parameters in the polymer are $U = 10t$, $V = t$, and $\delta = 0.2$, corresponding to the energy of the B_u exciton, $E_0 = 9.537t$ (indicated by the arrow). The dopant concentration $c = 0.2$. In the solid line, $v = 0.212t$, and in the dashed line, $v = 0.566t$.

$$F(\epsilon) = \frac{v^2}{J(1 - \delta^2)} \left(\sqrt{\frac{E + 2J(1 - \delta^2)}{E}} - 1 \right), \quad (5.15)$$

with

$$E = -(\epsilon + E_0 - \Delta_e - 2J\delta^2). \quad (5.16)$$

Figure 22 illustrates the probability of charge transfer to the dopant. The dopant concentration is set to be 0.2, a typical value for a molecularly doped polymer. We see that when the acceptor level is near the exciton energy E_0 , a crossover will occur. When the acceptor level is below this crossover value, the electron is mainly on the dopant. Otherwise, the electron is mainly on the polymer chain. The coupling strength v affects the charge transfer by controlling the width of the crossover. The smaller v is, the more rapid the crossover is.

For the A_g exciton, if we make the assumption $B_1^- = -B_{-1}^- = (1/\sqrt{2})$, then

$$|B_k| = \left| \sum_l B_l^- e^{ikl} \right| = \sqrt{2} \sin k, \quad (5.17)$$

and we have

$$F(\epsilon) = \frac{v^2}{J(1 - \delta^2)} \left(1 - \sqrt{\frac{E}{E + 2J(1 - \delta^2)}} \right). \quad (5.18)$$

We plot the charge transfer probability for the A_g state in Fig. 23. We can see that there is a threshold for Δ_e . Below this value, the electron will thoroughly transfer to the dopant molecule. However for the B_u state there is a long tail below the critical value, indicating some fraction of the electron can still be found in the polymer. Having gained the knowledge of how Δ_e , v , and the exciton wave function influence the probability of charge transfer, one will be able to control this transfer process in the conjugated polymer.

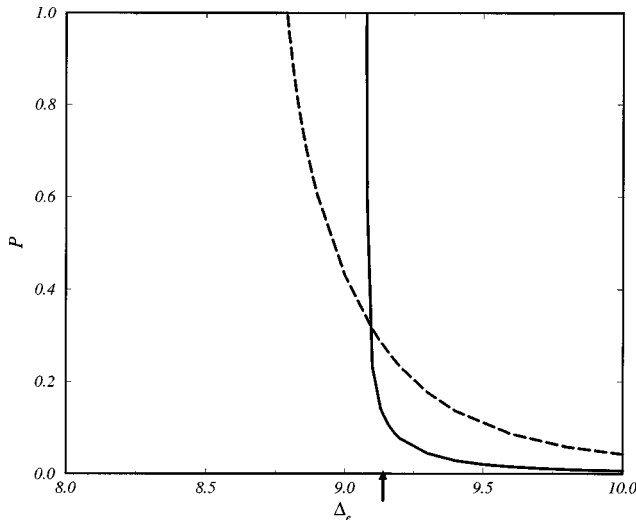


FIG. 23. Probability of charge transfer of the A_g state as a function of acceptor level Δ_e . The parameters are the same as those in Fig. 22, and the corresponding A_g state has energy $E_0=9.140t$ (indicated by the arrow). The solid and dashed lines correspond to $v=0.212t$ and $v=0.566t$, respectively.

VI. CONCLUDING REMARKS

In this paper, we have extensively studied the exciton states in conjugated polymers by emphasizing the dominant role of $e-e$ correlations. The model we studied here is the widely used Peierls-extended Hubbard model with frozen bond dimerization. First, in the large- U approximation, we mapped this model to a spinless fermion model with only nearest-neighbor Coulomb interaction in real space. The short-range interaction enabled us to apply t matrix theory to analytically calculate the energy spectrum and wave function of bound (exciton) states. We have found that there always exists a stable A_g exciton as long as the nearest-neighbor Coulomb V is nonzero; for the B_u state, however, a stable exciton state can exist only when V is larger than the half width of the continuum band. This criterion has been proven based on Levinson's theorem. In our results, we have a correct ordering for A_g and B_u states, i.e., $2A_g < 1B_u$, as observed in most conjugated polymers. The impurity effects on the coherent motion of the excitons were also investigated in this large- U approximation. The coherence of the exciton can be measured by an appropriately defined electron-hole correlation function. We have studied impurities with on-site potentials as well as a charged impurity with a more extended potential. There are three kinds of impurity with the on-site potential: the first is like a local charge, attracting holes but repelling electrons (or vice versa); the second acts as a well, attracting both electron and hole; the third is like a barrier which repels both electron and hole. We have found that for the first and second type of impurities, the electron-hole correlations exhibit a crossover when the impurity strength V_0 is comparable to the exciton bandwidth J , which describes the exciton being trapped by the impurity. For the second type of impurity, if the impurity strength is larger than the Coulomb interaction V , the deep well will trap the electron and hole separately, leading to the total decorrelation of the exciton as a particle. For the third type of impu-

rity, the exciton coherence can survive the impurity and the distribution in momentum space has a sharp peak which means the exciton still moves freely. For the charged impurity with an extended potential of range greater than l_V , the range of the Coulomb interaction, the free exciton becomes trapped at $V_0 \sim J$, analogous to the situation for on-site impurity potentials. However, unlike the charged impurity with the on-site potential, the exciton dissociates into an uncorrelated electron-hole pair when V_0 is sufficiently large compared to the Coulomb strength V .

We have also investigated the effects of interchain coupling and the resulting interchain exciton states within the strong correlation approximation by considering a two-chain system with nearest-neighbor interchain hopping t_\perp and Coulomb interaction V_\perp . In this coupled system, we have two conduction bands and two valence bands. Within the t matrix formalism, we have found six poles for every center-of-mass momentum K , in which two poles are determined solely by V_\perp , corresponding to interchain excitons, while the other four poles are determined solely by the intrachain Coulomb interaction V , corresponding to intrachain excitons. We have also illustrated the wave functions of the static interchain exciton. There is still some amplitude for the electron and hole being on the same chain for the interchain exciton state. For more complicated Coulomb potentials, we propose a way to distinguish the interchain and intrachain excitons, namely by comparing the interchain electron-hole correlation function with the intrachain one.

The charge transfer in a molecularly doped conjugated polymer has been studied by constructing a variational wave function for the whole system including the polymer chain and dopant molecule. We modeled this coupled system by simply regarding the molecule has an acceptor level which interacts with the polymer chain by nearest-neighbor hopping v . Minimizing the energy of the state, we have obtained the energy of the variational state and, accordingly, the probability of charge transfer. We have shown that a crossover behavior will occur when the acceptor level is near to the exciton energy. When the acceptor level is higher than this crossover value, the electron mainly remains on the polymer chain. Otherwise, most of the electron density will transfer to the dopant molecule. The hopping v controls the width of this crossover, the larger v is, the more gentle is the crossover. The wave function is also an important influence on the charge transfer. For the A_g state, there is a threshold for the acceptor level. If Δ_e is less than this value, the charge transfers to the molecule thoroughly and the percentage of electron density in the polymer chain is zero.

Our calculations in this paper presented a comprehensive picture of the exciton in conjugated polymers, in a limit in which the electron correlation effects have been taken seriously and consistently. Our exciton theory can be readily extended to a system with a relatively long range Coulomb interaction. Also using our spinless fermion representation for the Peierls-extended Hubbard model, biexciton states can be obtained either by the Heitler-London method or diagonalization of the Hamiltonian in two electron-hole pair space. Although for real conjugated polymers, the Hubbard U is not so strong and our results cannot quantitatively match the energy levels in luminescent polymers, our theory is useful for understanding several puzzles which have arisen from

correlation effects in conjugated polymers. Finally, we note that recent experimental evidence has demonstrated that there is an excitonic contribution to the pairing mechanism in $\text{YBa}_2\text{Cu}_3\text{O}_{7-\delta}$.⁵⁸ We expect that our exciton theory can give some guidance for exciton effects in high- T_c superconductors by extending the formalism to two dimensions.

ACKNOWLEDGMENTS

We are grateful to X. Sun, Z. Shuai, W. Z. Wang, J. T. Gammel, S. A. Brazovskii, N. N. Kirova, S. Mazundar, Z. G. Soos, and D. Schmeltzer for many helpful discussions and criticisms. This work was supported by the U.S. Department of Energy.

APPENDIX A: EXPLICIT EXPRESSIONS OF GREEN'S FUNCTIONS

In this Appendix, we will give explicit expressions for $G(0;E_0)$ and $G(2;E_0)$ in different energy regions, calculated according to the definition Eq. (2.35). Here we use the same notation as in the text; $x = E_G - E_0$. When $E_0 > E_f$, i.e., $x < -4J(1 + \delta^2)$, the energy is above the top of the continuum band, and the Green's functions are

$$G(0;E_0) = \frac{1}{\sqrt{x^2 - 4J(1 + \delta^2)|x|}}, \quad (\text{A1})$$

$$G(2;E_0) = -\frac{1}{2J(1 + \delta^2)} + \left[\frac{|x|}{2J(1 + \delta^2)} - 1 \right] \times \frac{1}{\sqrt{x^2 - 4J(1 + \delta^2)|x|}}. \quad (\text{A2})$$

When $E_i < E_0 < E_f$, i.e., $-4J(1 + \delta^2) < x < 0$, the energy is within the continuum band,

$$G(0;E_0) = -i \frac{1}{\sqrt{-x^2 - 4J(1 + \delta^2)x}}, \quad (\text{A3})$$

$$G(2;E_0) = -\frac{1}{2J(1 + \delta^2)} + i \left[\frac{x}{2J(1 + \delta^2)} + 1 \right] \times \frac{1}{\sqrt{-x^2 - 4J(1 + \delta^2)x}}. \quad (\text{A4})$$

When $E_0 < E_i$, i.e., $x > 0$, the energy is in the gap,

$$G(0;E_0) = -\frac{1}{\sqrt{x^2 + 4J(1 + \delta^2)x}}, \quad (\text{A5})$$

$$G(2;E_0) = -\frac{1}{2J(1 + \delta^2)} + \left[\frac{x}{2J(1 + \delta^2)} + 1 \right] \times \frac{1}{\sqrt{x^2 + 4J(1 + \delta^2)x}}. \quad (\text{A6})$$

APPENDIX B: DIAGONALIZATION OF HAMILTONIAN (4.4)

Hamiltonian (4.4) can be written as

$$\begin{aligned} \tilde{H}_0 = & \sum_k (\eta_{1k}^\dagger \eta_{2k}^\dagger) \begin{pmatrix} \epsilon_k & t_\perp \\ t_\perp & \epsilon_k \end{pmatrix} \begin{pmatrix} \eta_{1k} \\ \eta_{2k} \end{pmatrix} + \sum_k (\gamma_{1k}^\dagger \gamma_{2k}^\dagger) \\ & \times \begin{pmatrix} \tilde{\epsilon}_k & -t_\perp \\ -t_\perp & \tilde{\epsilon}_k \end{pmatrix} \begin{pmatrix} \gamma_{1k} \\ \gamma_{2k} \end{pmatrix}. \end{aligned} \quad (\text{B1})$$

Making the transformations

$$\begin{pmatrix} \eta_{1k} \\ \eta_{2k} \end{pmatrix} = \frac{1}{\sqrt{2}} \begin{pmatrix} 1 & 1 \\ -1 & 1 \end{pmatrix} \begin{pmatrix} \tilde{\eta}_{1k} \\ \tilde{\eta}_{2k} \end{pmatrix} \quad (\text{B2})$$

and

$$\begin{pmatrix} \gamma_{1k} \\ \gamma_{2k} \end{pmatrix} = \frac{1}{\sqrt{2}} \begin{pmatrix} 1 & -1 \\ 1 & 1 \end{pmatrix} \begin{pmatrix} \tilde{\gamma}_{1k} \\ \tilde{\gamma}_{2k} \end{pmatrix}, \quad (\text{B3})$$

we have

$$\tilde{H}_0 = \sum_{lk} (E_k^l \tilde{\eta}_{lk}^\dagger \tilde{\eta}_{lk} + \tilde{E}_k^l \tilde{\gamma}_{lk}^\dagger \tilde{\gamma}_{lk}) \quad (\text{B4})$$

and the relation between the two types of local operators η_{il} (γ_{il}) and $\tilde{\eta}_{il}$ ($\tilde{\gamma}_{il}$):

$$\eta_{1l} = \frac{1}{\sqrt{2}} (\tilde{\eta}_{1l} + \tilde{\eta}_{2l}), \quad (\text{B5})$$

$$\eta_{2l} = \frac{1}{\sqrt{2}} (-\tilde{\eta}_{1l} + \tilde{\eta}_{2l}), \quad (\text{B6})$$

$$\gamma_{1l} = \frac{1}{\sqrt{2}} (\tilde{\gamma}_{1l} - \tilde{\gamma}_{2l}), \quad (\text{B7})$$

$$\gamma_{2l} = \frac{1}{\sqrt{2}} (\tilde{\gamma}_{1l} + \tilde{\gamma}_{2l}). \quad (\text{B8})$$

¹J. H. Burroughes *et al.*, Nature (London) **347**, 539 (1990).

²D. Braun and A. J. Heeger, Appl. Phys. Lett. **58**, 1982 (1991).

³P. L. Burn *et al.*, Nature (London) **356**, 47 (1992).

⁴M. Berggren *et al.*, Nature (London) **372**, 444 (1994).

⁵A. R. Brown *et al.*, Appl. Phys. Lett. **61**, 2793 (1992).

⁶G. Gustafsson *et al.*, Nature (London) **357**, 477 (1992).

⁷A. J. Heeger, S. Kivelson, J. R. Schrieffer, and W. P. Su, Rev. Mod. Phys. **60**, 781 (1988).

⁸*Nonlinear Optical Properties of Organic Molecules and Crystals*, edited by D. S. Chemla and J. Zyss (Academic, New York, 1987), Vol. 2.

⁹M. Chandross *et al.*, Phys. Rev. B **50**, 14 702 (1994).

- ¹⁰P. Gomes da Costa and E. M. Conwell, Phys. Rev. B **48**, 1993 (1993).
- ¹¹Z. Shuai, J. L. Brédas, and W. P. Su, Chem. Phys. Lett. **228**, 301 (1994).
- ¹²Z. G. Yu *et al.*, Phys. Rev. B **52**, 4849 (1995).
- ¹³J. Frenkel, Phys. Rev. **17**, 17 (1931).
- ¹⁴S. Suhai, Phys. Rev. B **29**, 4570 (1984).
- ¹⁵H. Hayashi and K. Nasu, Phys. Rev. B **32**, 5295 (1985).
- ¹⁶H. Tanaka, M. Inoue, and E. Hanamura, Solid State Commun. **63**, 103 (1987).
- ¹⁷S. Abe, J. Yu, and W. P. Su, Phys. Rev. B **45**, 8264 (1992).
- ¹⁸See, for example, S. Nakajima, Y. Toyozawa, and R. Abe, *The Physics of Elementary Excitations* (Springer-Verlag, Berlin, 1980).
- ¹⁹P. E. Peierls, *Quantum Theory of Solids* (Clarendon, Oxford, 1955).
- ²⁰A. A. Ovchinnikov, I. I. Ukrainskii, and G. V. Kventsel, Usp. Fiz. Nauk **108**, 81 (1972) [Sov. Phys. Usp. **15**, 575 (1973)].
- ²¹I. I. Ukrainskii, Zh. Eksp. Teor. Fiz. **76**, 760 (1979) [Sov. Phys. JETP **49**, 381 (1979)].
- ²²D. Baeriswyl and K. Maki, Phys. Rev. B **31**, 6633 (1985); Synth. Met. **17**, 13 (1987).
- ²³C. Wu, X. Sun, and K. Nasu, Phys. Rev. Lett. **59**, 831 (1987); X. Sun, Z. Shuai, K. Nasu, D. L. Lin, and T. F. George, Phys. Rev. B **44**, 11 042 (1991).
- ²⁴Z. Shuai, Synth. Met. **85**, 1011 (1997).
- ²⁵D. Guo *et al.*, Phys. Rev. B **48**, 1433 (1993).
- ²⁶Z. G. Soos, S. Etemad, D. S. Galvão, and S. Ramasesha, Chem. Phys. Lett. **194**, 341 (1992); Z. G. Soos, S. Ramasesha, D. S. Galvão, and S. Etemad, Phys. Rev. B **47**, 1742 (1993).
- ²⁷S. Mazumdar *et al.*, J. Chem. Phys. **104**, 9283 (1996).
- ²⁸F. Guo, M. Chandross, and S. Mazumdar, Phys. Rev. Lett. **74**, 2086 (1995).
- ²⁹E. Abrahams, P. W. Anderson, D. C. Licciardello, and T. V. Ramakrishnan, Phys. Rev. Lett. **42**, 673 (1979).
- ³⁰D. Baeriswyl and K. Maki, Phys. Rev. B **24**, 2068 (1983).
- ³¹H. A. Mizes and E. M. Conwell, Phys. Rev. Lett. **70**, 1505 (1993).
- ³²J. W. P. Hsu, M. Yan, T. M. Jedju, and L. J. Rothberg, Phys. Rev. B **49**, 712 (1994).
- ³³M. Yan *et al.*, Phys. Rev. Lett. **72**, 1104 (1994); **73**, 744 (1994).
- ³⁴M. Yan, L. J. Rothberg, E. W. Kwock, and T. M. Miller, Phys. Rev. Lett. **75**, 1992 (1995).
- ³⁵H. A. Mizes and E. M. Conwell, Phys. Rev. B **50**, 11 243 (1994).
- ³⁶Z. G. Yu *et al.*, J. Phys. Condens. Matter **8**, 8847 (1996).
- ³⁷N. S. Sariciftci *et al.*, Science **258**, 1474 (1992).
- ³⁸R. G. Kepler and P. A. Cahill, Appl. Phys. Lett. **63**, 1552 (1993).
- ³⁹M. J. Rice and Yu. N. Gartstein, Phys. Rev. B **53**, 10 764 (1996).
- ⁴⁰D. Baeriswyl, D. K. Campbell, and S. Mazumdar, in *Conjugated Conducting Polymers*, edited by H. Kiess (Springer, Berlin, 1992), pp. 7–133, and references therein.
- ⁴¹Z. G. Soos, Annu. Rev. Phys. Chem. **25**, 121 (1974).
- ⁴²J. M. Leng *et al.*, Phys. Rev. Lett. **72**, 156 (1994).
- ⁴³N. F. Colaneri *et al.*, Phys. Rev. B **42**, 11 670 (1990).
- ⁴⁴M. Gailberger and H. Bässler, Phys. Rev. B **44**, 8643 (1991).
- ⁴⁵U. Rauscher, H. Bässler, D. D. C. Bradley, and M. Hennecke, Phys. Rev. B **42**, 9830 (1990).
- ⁴⁶D. Beljonne, Z. Shuai, R. H. Friend, and J. L. Brédas, J. Chem. Phys. **102**, 2042 (1995).
- ⁴⁷E. H. Lieb and F. Y. Wu, Phys. Rev. Lett. **20**, 1445 (1968).
- ⁴⁸Z. Y. Weng, D. N. Sheng, C. S. Ting, and Z. B. Su, Phys. Rev. B **45**, 7850 (1992).
- ⁴⁹An exact diagonalization for a short chain ($N=6$) with the parameters $V=t$ and $\delta=0.2$ has been carried out, W. Z. Wang (unpublished). We found that splittings between the lowest singlet and triplet exciton states are $0.034t$ for $U=10t$, $0.016t$ for $U=8t$, and $0.14t$ for $U=6t$.
- ⁵⁰See, for example, J. Callaway, *Quantum Theory of the Solid State*, 2nd ed. (Academic, San Diego, 1991).
- ⁵¹Z. Shuai (private communication).
- ⁵²R. G. Newton, *Scattering Theory of Particles and Waves* (McGraw-Hill, New York, 1966).
- ⁵³B. E. Kohler, C. Spangler, and C. Westerfield, J. Chem. Phys. **89**, 5422 (1988).
- ⁵⁴B. S. Hudson, B. E. Kohler, and K. Schulten, in *Excited States*, edited by E. C. Lim (Academic, New York, 1982), pp. 1–95.
- ⁵⁵R. H. McKenzie and J. W. Wilkins, Phys. Rev. Lett. **69**, 1085 (1992).
- ⁵⁶S. R. Phillpot, D. Baeriswyl, A. R. Bishop, and P. S. Lomdahl, Phys. Rev. B **35**, 7533 (1987).
- ⁵⁷See, for example, A. A. Abrikosov, L. P. Gorkov, and I. E. Dzialoshinskii, *Methods of Quantum Field Theory in Statistical Physics* (Pergamon Press, Oxford, 1965).
- ⁵⁸M. J. Holcomb *et al.*, Phys. Rev. Lett. **73**, 2360 (1994).